



Universitat  
d'Alacant



GOBIERNO  
DE ESPAÑA

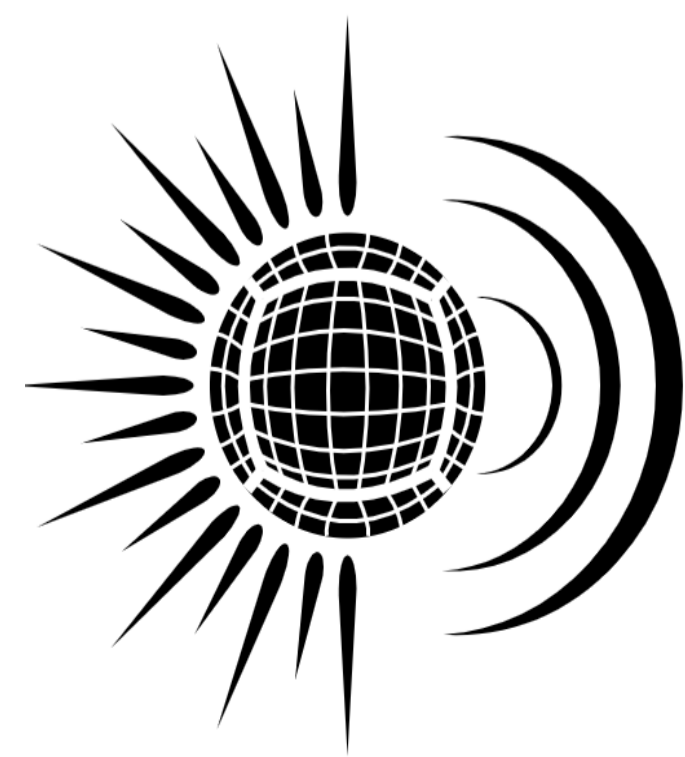
MINISTERIO  
DE CIENCIA  
E INNOVACIÓN



GENERALITAT  
VALENCIANA

Conselleria de Educació, Cultura,  
Universitats y Empleo

# Magnetic and thermal evolution of neutron stars with superfluid and superconducting interiors



**MATINS**

MAgneto-Thermal evolution  
of Isolated Neutron Stars

June 24, 2026

Scales General Meeting

University of Coimbra, Portugal

**Clara Dehman**

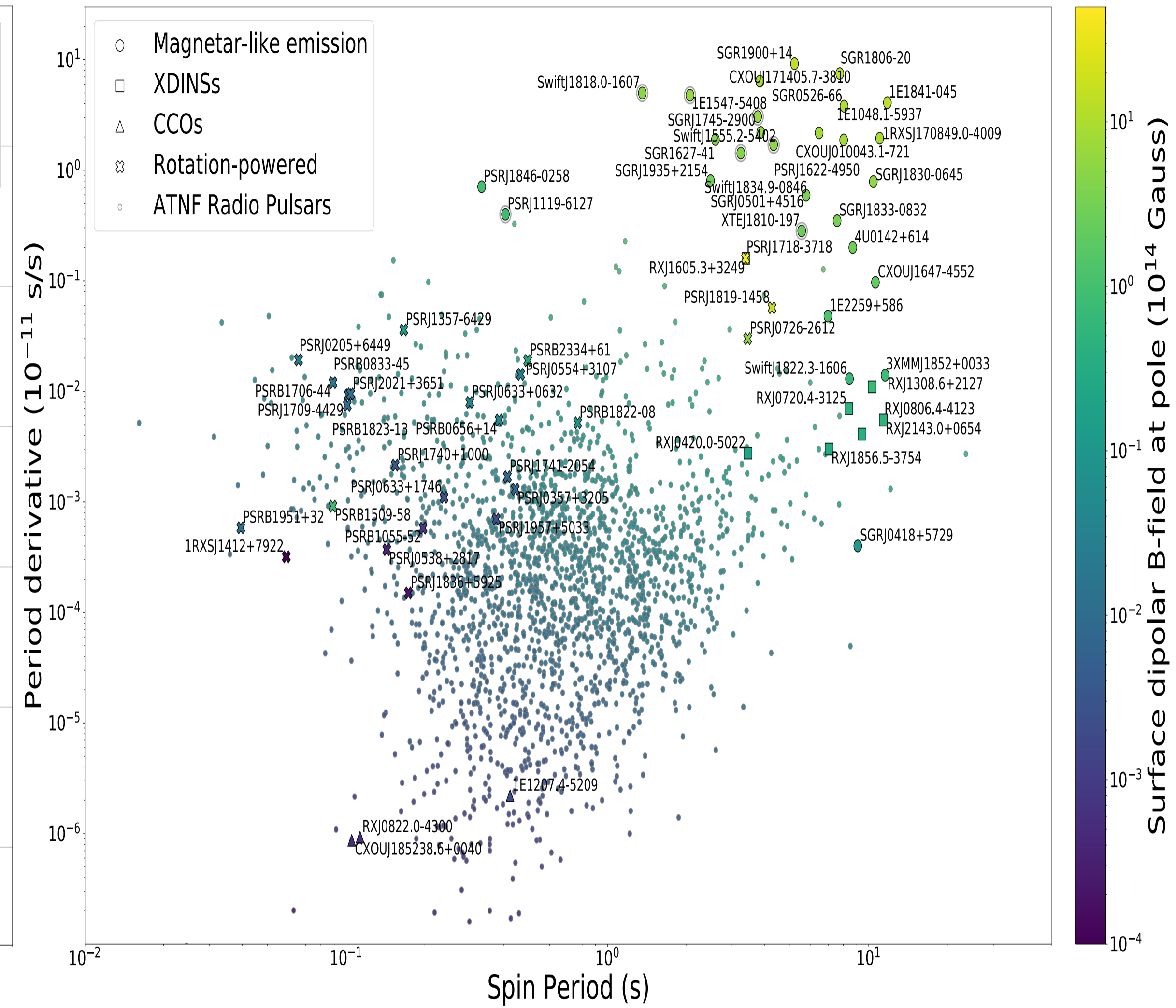
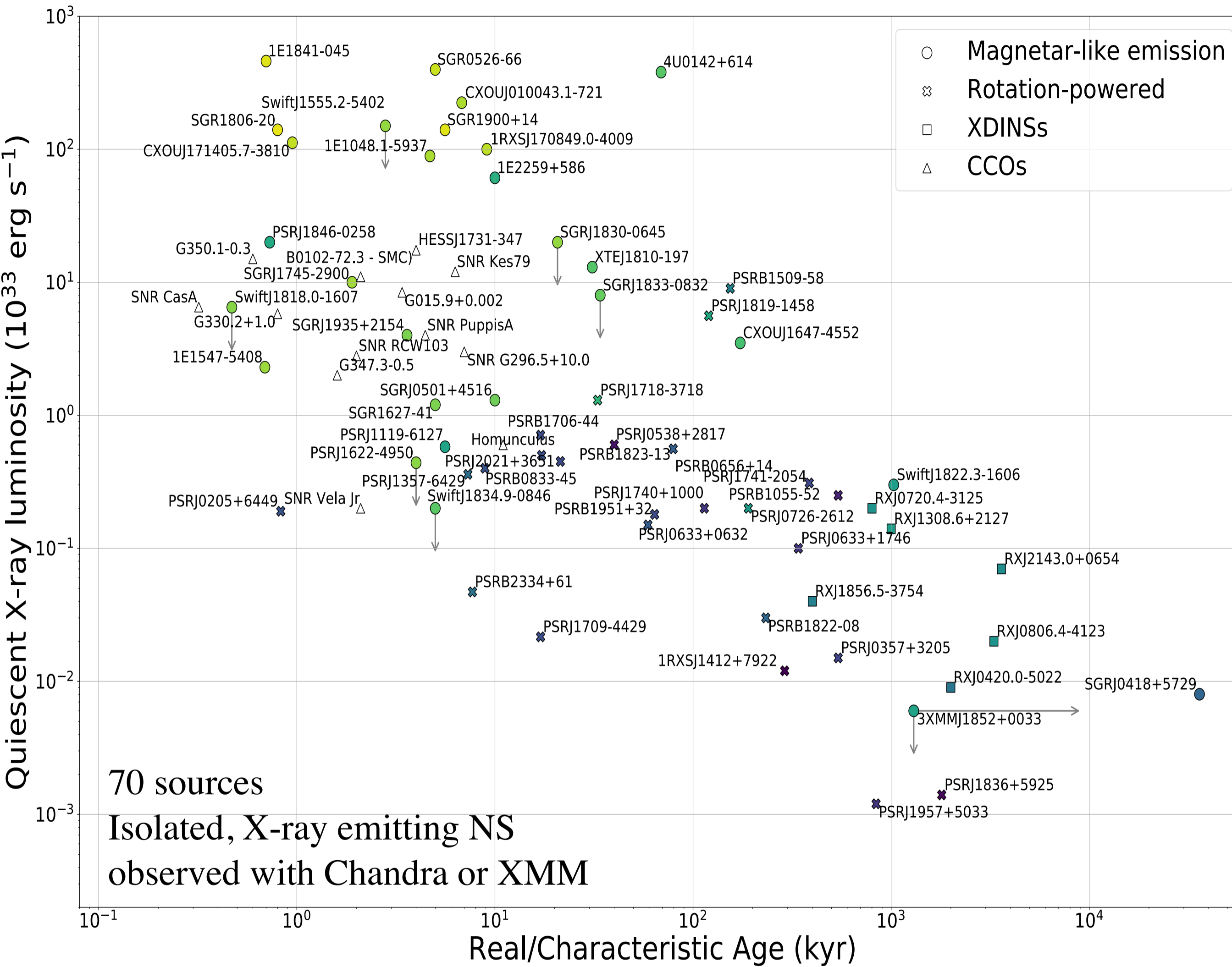
[clara.dehman@ua.es](mailto:clara.dehman@ua.es)

Juan de la Cierva Fellow





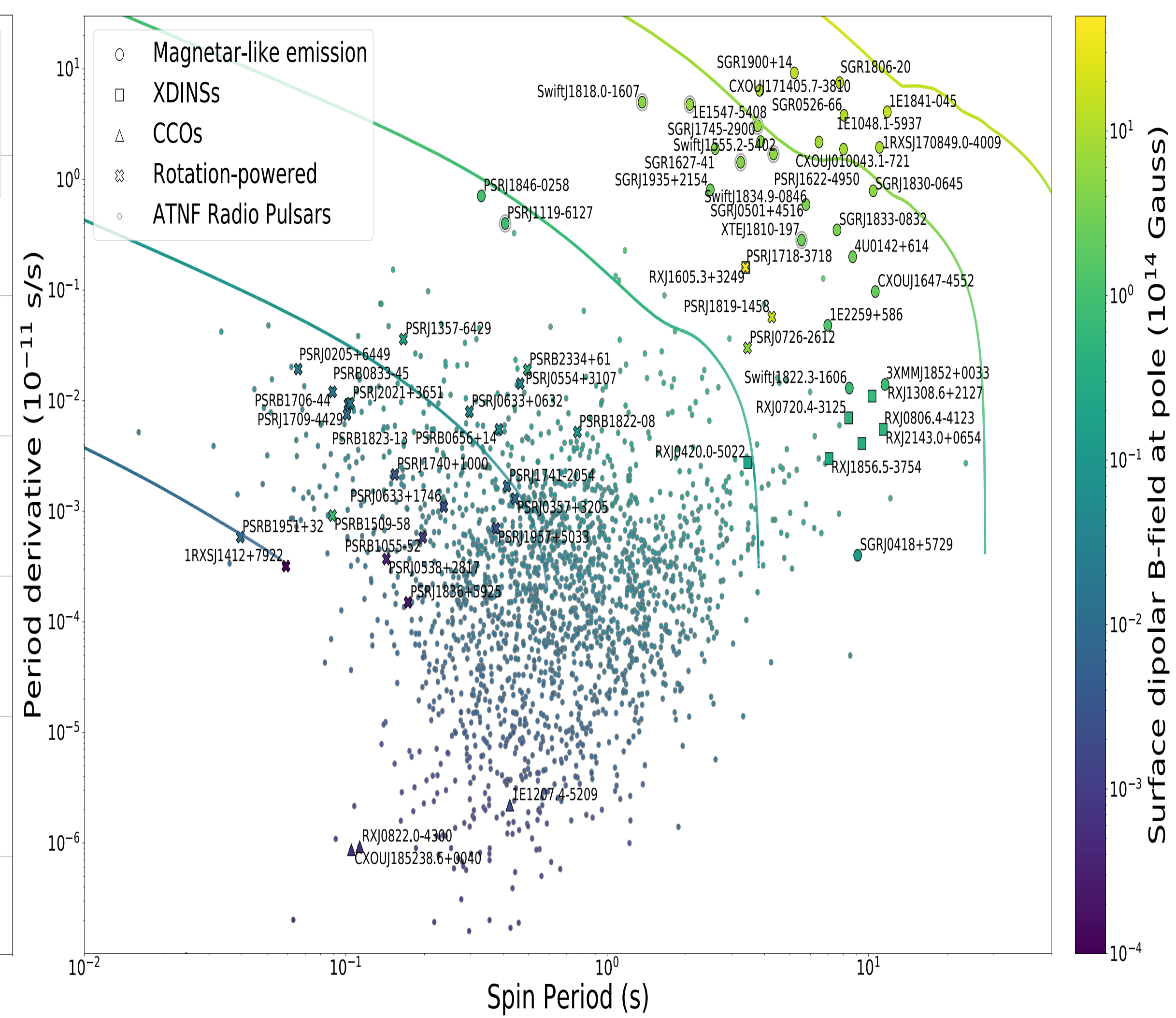
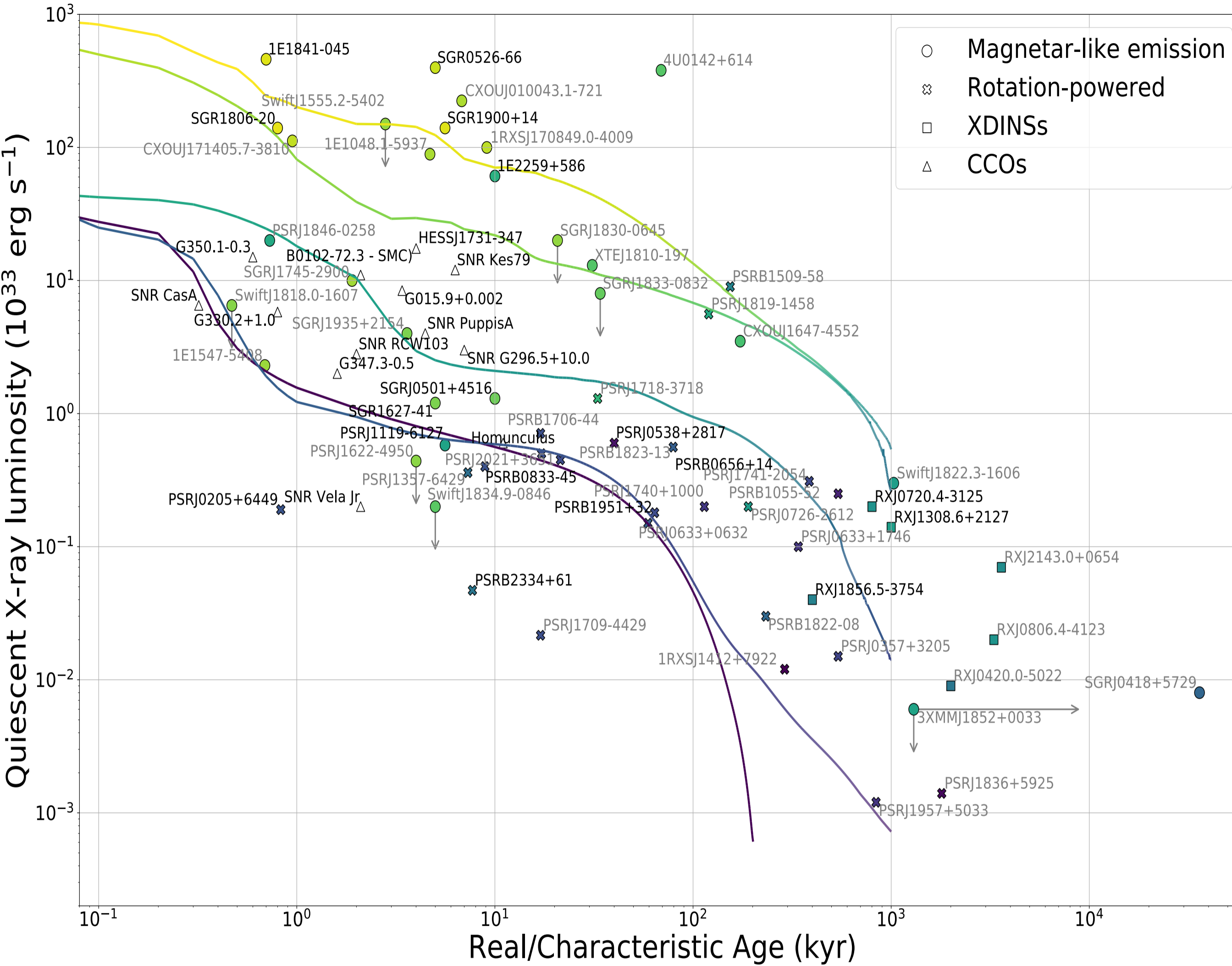
# Observations: thermal X-ray luminosity, real age, P and Pdot



**Four independent measured parameters.**

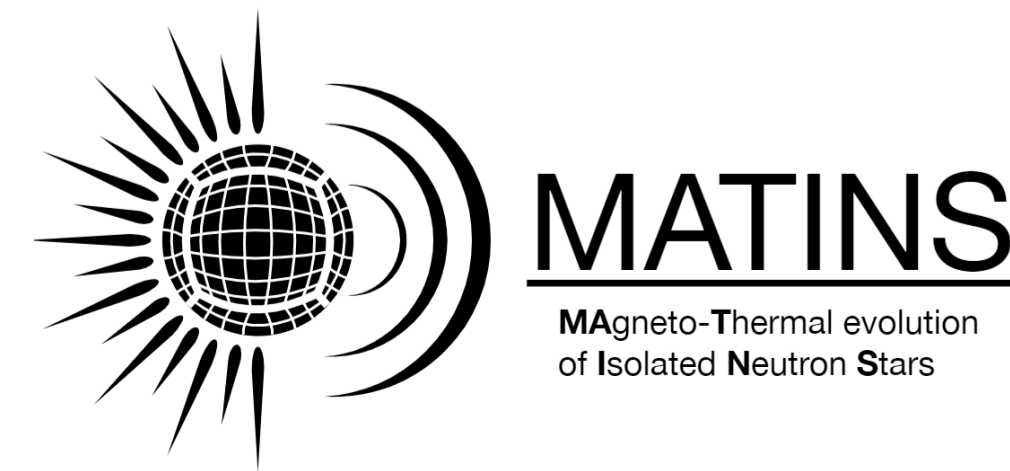
*“Need for coupled magneto-thermal simulations to explain the luminosity and the evolution path of different isolated neutron stars” — [Viganò et al. 2013].*

# Why we need 3D magneto-thermal models?



- Realistic magnetic topology: complex and non-axisymmetric
- The need to model cooling curves, that depend on the 3d configuration

*“New 3D code  
 MATINS”*



# Neutron star model & Cooling

The structure is provided by the TOV equations which solve the hydrostatic equilibrium assuming a static interior Schwarzschild metric

Cold matter EOS + central pressure: star structure & composition (fixed)

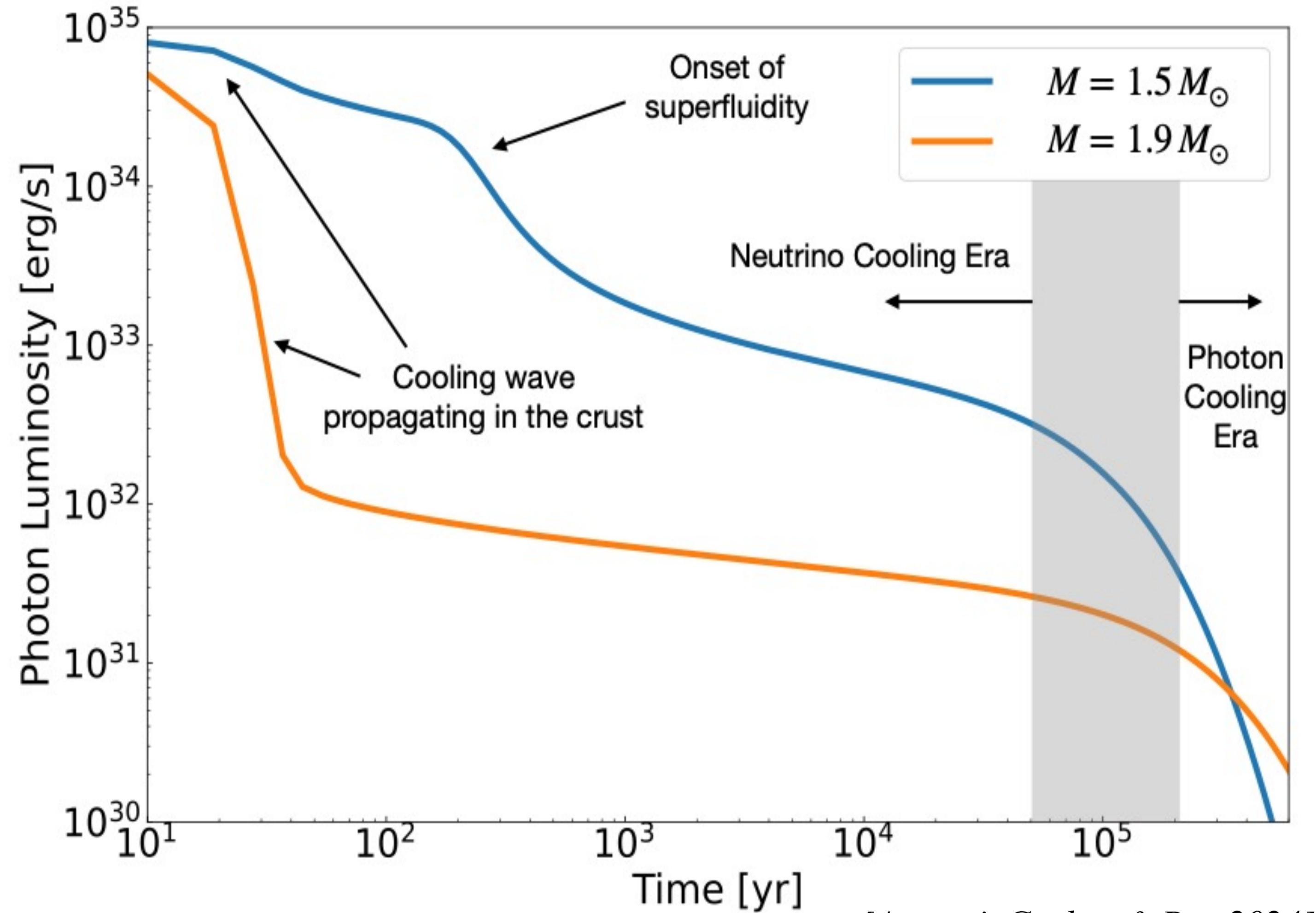
## Thermal evolution:

$$c_V(T) \frac{\partial(Te^\nu)}{\partial t} = \vec{\nabla} \cdot (e^\nu \hat{k} \cdot \vec{\nabla}(e^\nu T)) + e^{2\nu}(Q_J - Q_\nu)$$

## Ingredients:

- Heat capacity  $C_V(\rho, T)$ : main contribution by neutrons in the core
- **Thermal conductivity**  $\kappa(\rho, T, \mathbf{B})$  very large (star core rapidly isothermal), dominated by electrons, becomes **anisotropic** in presence of magnetic field
- Neutrino emissivity  $Q_\nu(\rho, T, \mathbf{B})$
- Sources of internal heat  $Q_j$ : nuclear reactions, **Ohmic dissipation**, accretion...
- Hydrostatic equilibrium models of envelope (i.e., liquid outermost 100 m), that due to its stronger gradients of density and temperature has much faster timescales than the interior
- Emission model (atmosphere, **blackbody**, condensed surface...)

# Cooling Model: Neutrino vs Photon Cooling Stages



[Ascenzi, Graber & Rea 2024]

**Neutrino cooling dominates during the first 10-100 kyr: the star cools from inside.**

**Photon cooling dominates when the star is cold enough, so that neutrino production is much less efficient, and heat is mostly transferred to the surface and radiated.**

**Isolated neutron stars are X-ray bright because they are born hot, visible as thermal emitters.**

**For magnetars at least, need for extra heating.**

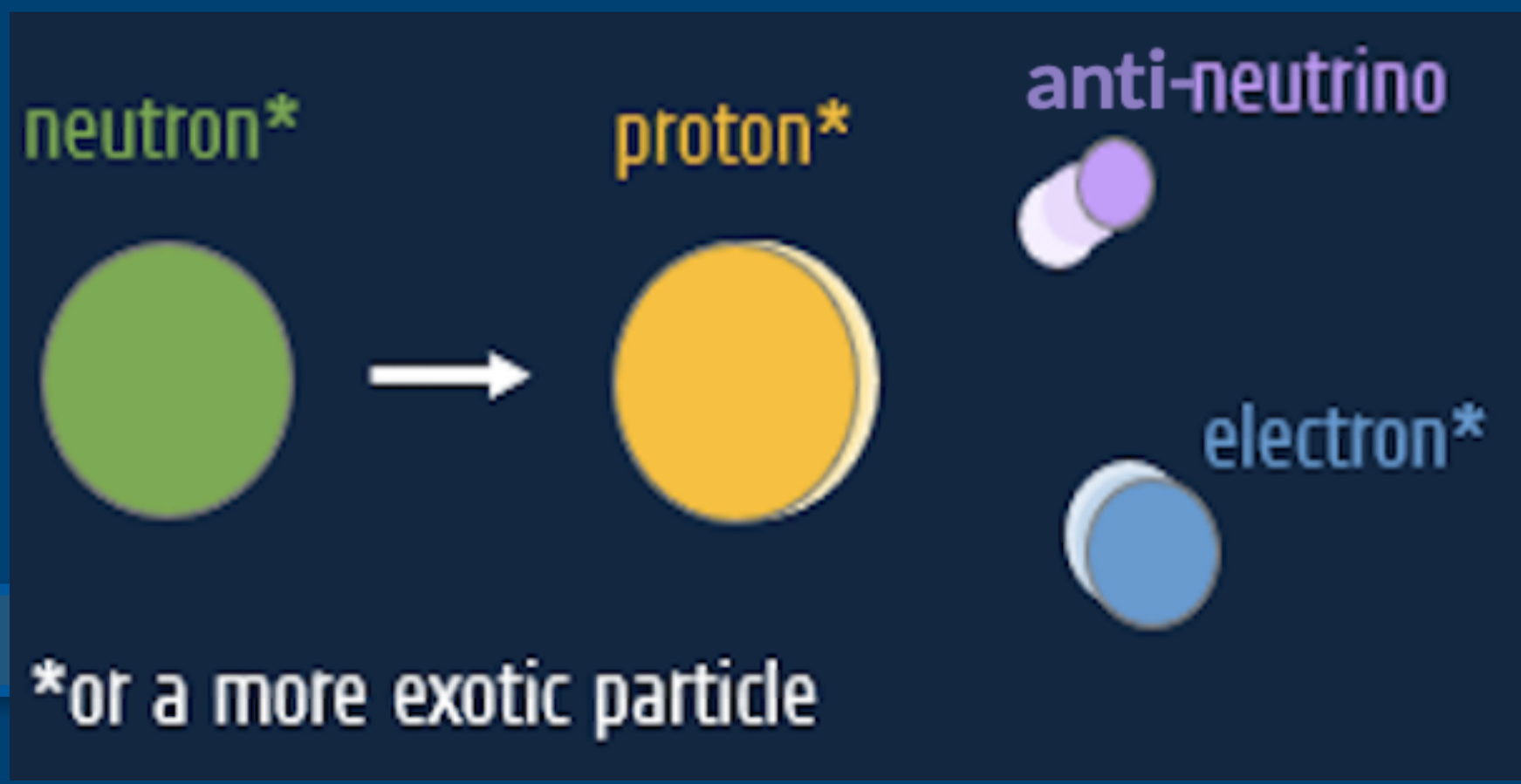
# Neutrinos Reactions



## Standard Cooling

+

## Enhanced Cooling



Process	$Q_\nu$ [erg cm <sup>-3</sup> s <sup>-1</sup> ]	Onset
<b>Core</b>		
Modified Urca (n-branch) $nn \rightarrow pne\bar{\nu}_e, pne \rightarrow nn\nu_e$	$8 \times 10^{21} \mathcal{R}_n^{MU} n_p^{1/3} T_9^8$	
Modified Urca (p-branch) $np \rightarrow ppe\bar{\nu}_e, ppe \rightarrow np\nu_e$	$8 \times 10^{21} \mathcal{R}_p^{MU} n_p^{1/3} T_9^8$	$Y_p^c = 0.01$
N-N bremsstrahlung $nn \rightarrow nn\nu\bar{\nu}$ $np \rightarrow np\nu\bar{\nu}$ $pp \rightarrow pp\nu\bar{\nu}$	$7 \times 10^{19} \mathcal{R}^{nn} n_n^{1/3} T_9^8$ $1 \times 10^{20} \mathcal{R}^{np} n_p^{1/3} T_9^8$ $7 \times 10^{19} \mathcal{R}^{pp} n_p^{1/3} T_9^8$	
e-p Bremsstrahlung $ep \rightarrow ep\nu\bar{\nu}$	$2 \times 10^{17} n_B^{-2/3} T_9^8$	
Direct Urca $n \rightarrow pe\bar{\nu}_e, pe \rightarrow n\nu_e$ $n \rightarrow p\mu^-\bar{\nu}_\mu, p\mu^- \rightarrow n\nu_\mu$	$4 \times 10^{27} \mathcal{R}^{DU} n_e^{1/3} T_9^6$ $4 \times 10^{27} \mathcal{R}^{DU} n_\mu^{1/3} T_9^6$	$Y_p^c = 0.11$ $Y_p^c = 0.14$
<b>Crust</b>		
Pair annihilation $ee^+ \rightarrow \nu\bar{\nu}$	$9 \times 10^{20} F_{\text{pair}}(n_e, n_{e^+})$	
Plasmon decay $\Gamma \rightarrow \nu + \bar{\nu}$	$1 \times 10^{20} I_{pl}(T, y_e)$	
e-nucleus Bremsstrahlung $e(A, Z) \rightarrow e(A, Z)\nu\bar{\nu}$	$3 \times 10^{12} L_{eN} Z \rho_0 n_e T_9^6$	
N-N Bremsstrahlung $nn \rightarrow nn\nu\bar{\nu}$	$7 \times 10^{19} R^{nn} f_\nu n_n^{1/3} T_9^8$	
<b>Core and crust</b>		
Cooper Pair Breaking and Formation (CPBF) $\tilde{B}\tilde{B} \rightarrow \nu\bar{\nu}$	$1 \times 10^{21} n_N^{1/3} F_{A,B} T_9^7$	
Electron Synchrotron $e \xrightarrow{B} e\nu\bar{\nu}$	$9 \times 10^{14} S_{AB,BC} B_{13}^2 T_9^5$	

# Impact of superfluidity and superconductivity on cooling

Different gap models strongly affect NS cooling, with the impact set by their height and width. In the zero-temperature limit, BCS theory predicts that the energy gaps are proportional to the critical temperature.

For the singlet (isotropic) pairing:

$$k_b T_c \approx 0.5669 \Delta,$$

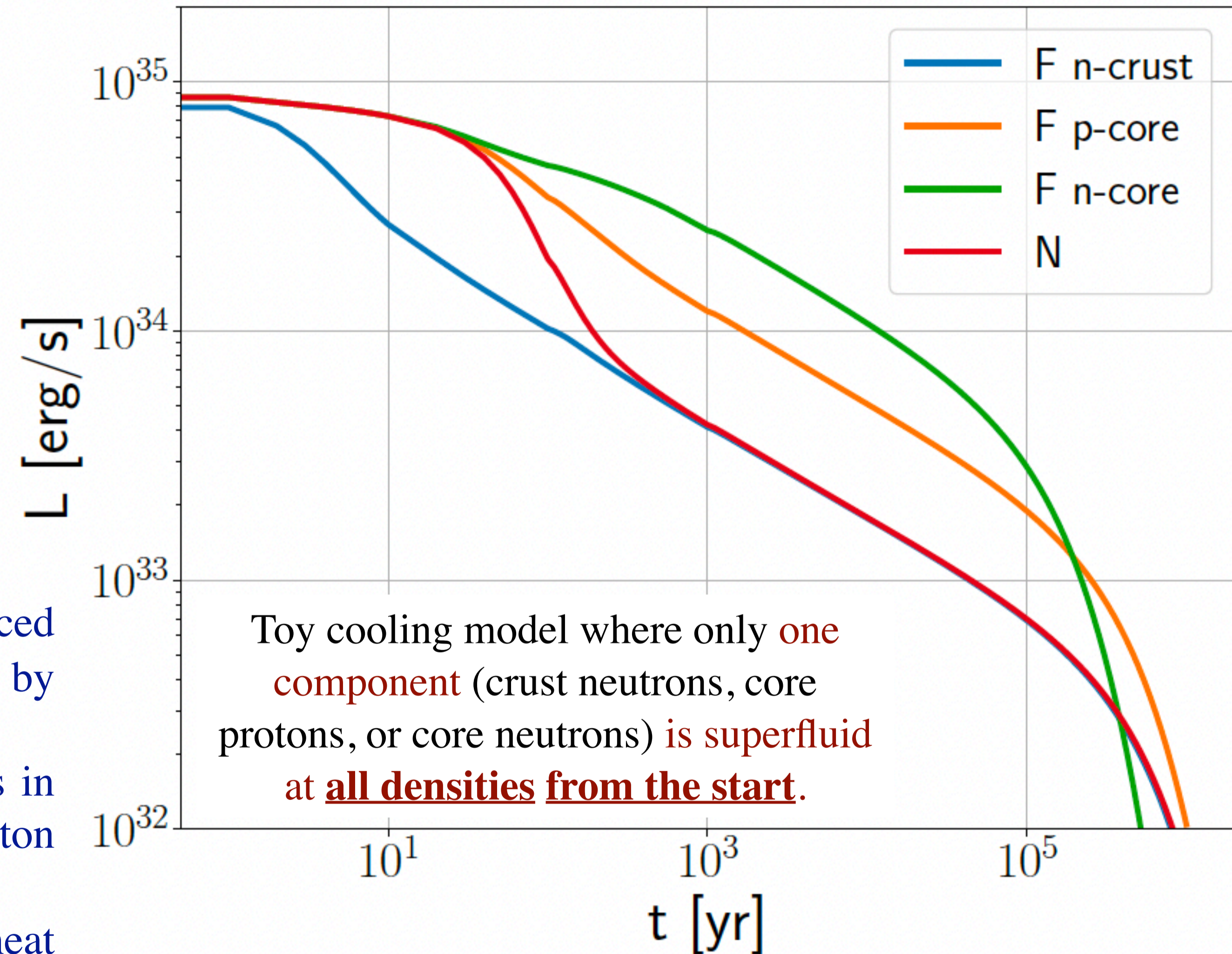
For the triplet (anisotropic) pairing

$$k_b T_c \approx 0.1887 \Delta,$$

[Ho et al. 2015]

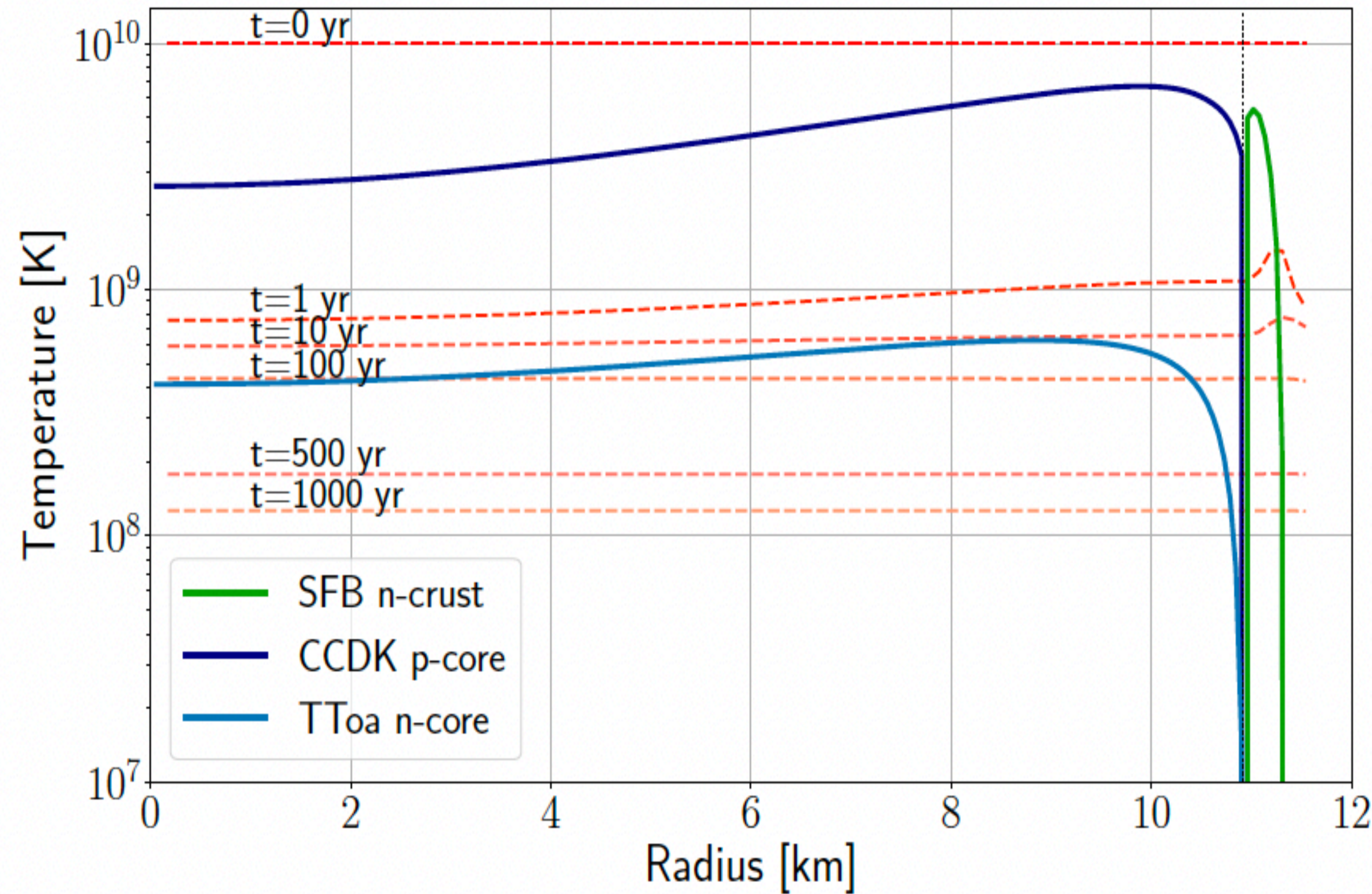
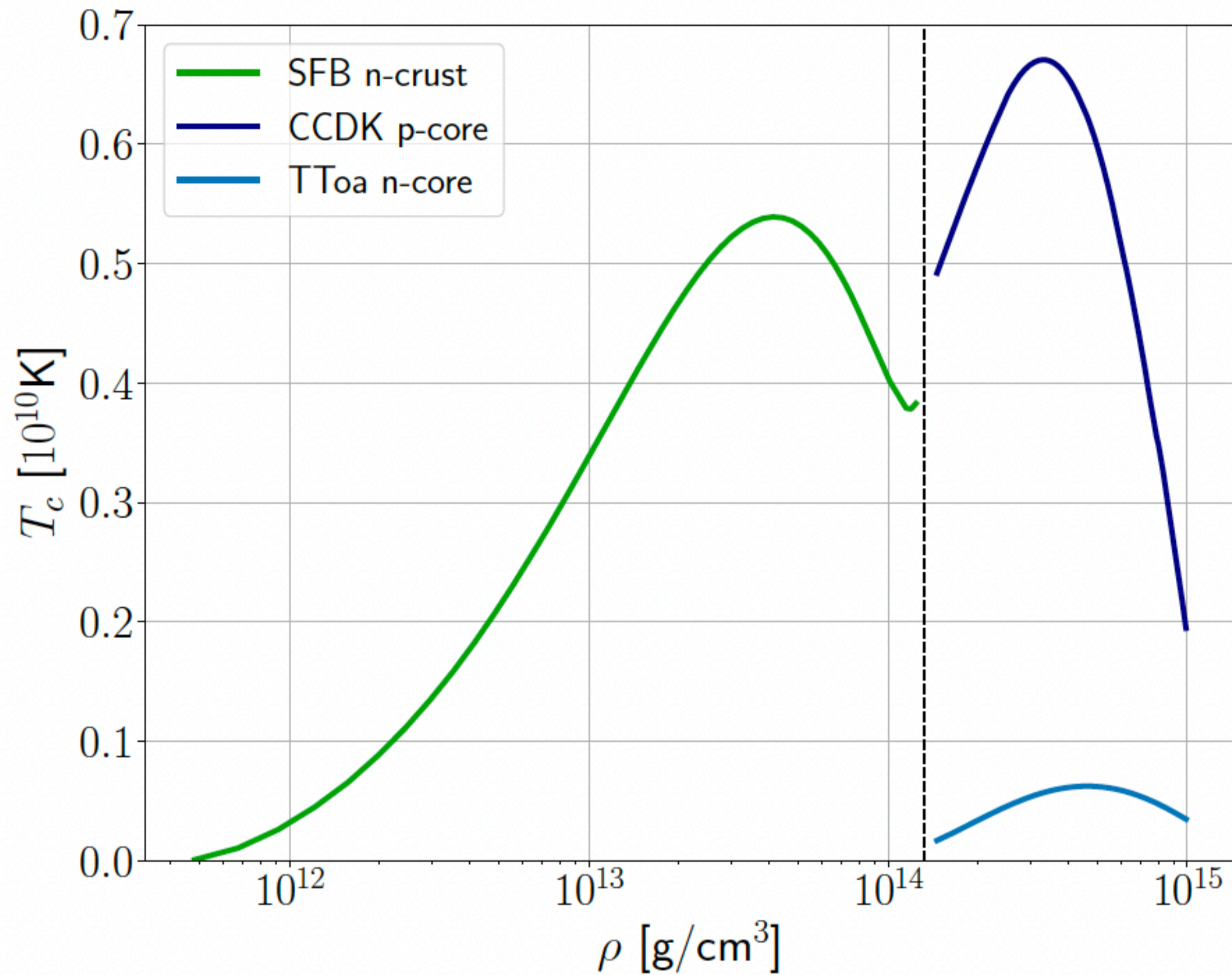
Higher critical temperature  $\rightarrow$  earlier superfluidity;  
Wider gap  $\rightarrow$  larger volume where transport is affected.

- 1) Early Evolution: onset of superfluidity ( $T \sim T_c$ )  $\rightarrow$  enhanced cooling from Cooper pair neutrino emission, mainly driven by crustal neutron superfluidity.
- 2) Mid evolution: suppression of standard neutrino processes in the core  $\rightarrow$  slower cooling, driven by neutron and proton superfluidity in the core.
- 3) Late time: fully superfluid regime ( $T \ll T_c$ )  $\rightarrow$  reduced heat capacity, so the star reacts faster to energy losses. Driven mainly by core neutron superfluidity.



# Gap models used in our current cooling models

**SF081326:** weak n-crust singlet gap (SFB); strong p-core singlet (CCDK); moderate n-core triplet (TToa).



## SF081326 evolution:

- Superfluidity when  $T < T_c$ .
- Early (weeks–months): p-core + n-crust become superfluid.
- Later ( $\sim 100$  yrs): n-core becomes superfluid.
- $\sim 100$  yrs: star becomes isothermal (end of thermal relaxation).
- Core superfluid volume  $\gg$  crust.

Marco Ermolli (Master's thesis)

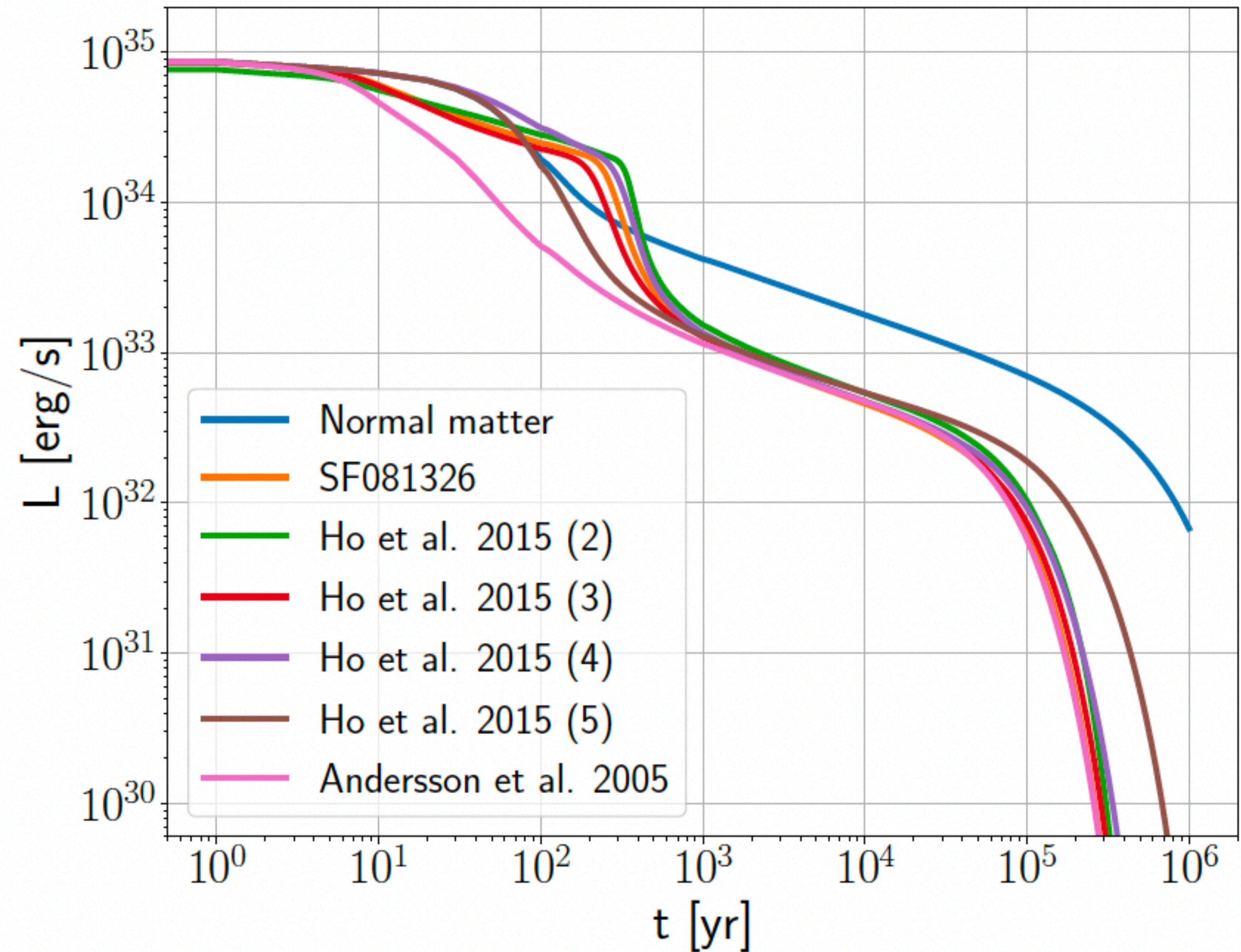
# Impact of superfluidity and superconductivity on cooling

Realistic gaps are density-dependent; their height and shape (uncertain) set where superfluid transitions occur.

The stronger the pairing (larger gap  $\Delta$ ), the higher the temperature at which the system becomes superfluid/superconducting.

Real stars show overlapping superfluid transitions, with competing effects that evolve as the star cools.

**Overall, superfluidity leads to faster cooling (BUT NOT enhanced cooling!) than normal matter.**

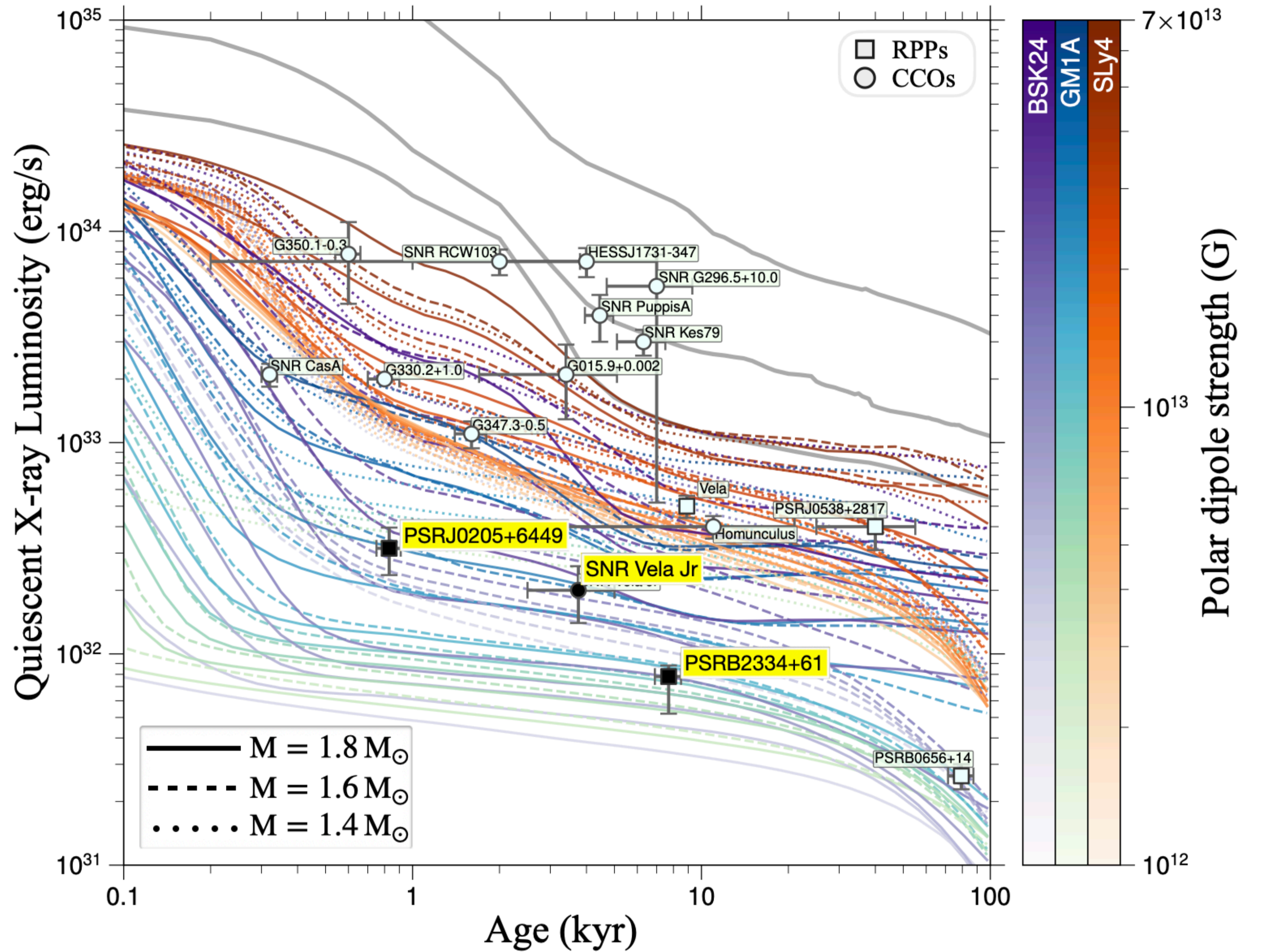


# Enhanced cooling and constraining nuclear EoS

This marks the first direct measurement of enhanced cooling. Magneto-thermal simulation and machine learning techniques were used to understand this finding.

A suitable EoS should elucidate both exceptionally bright objects like magnetars (Joule heating) and extremely faint objects at young ages.

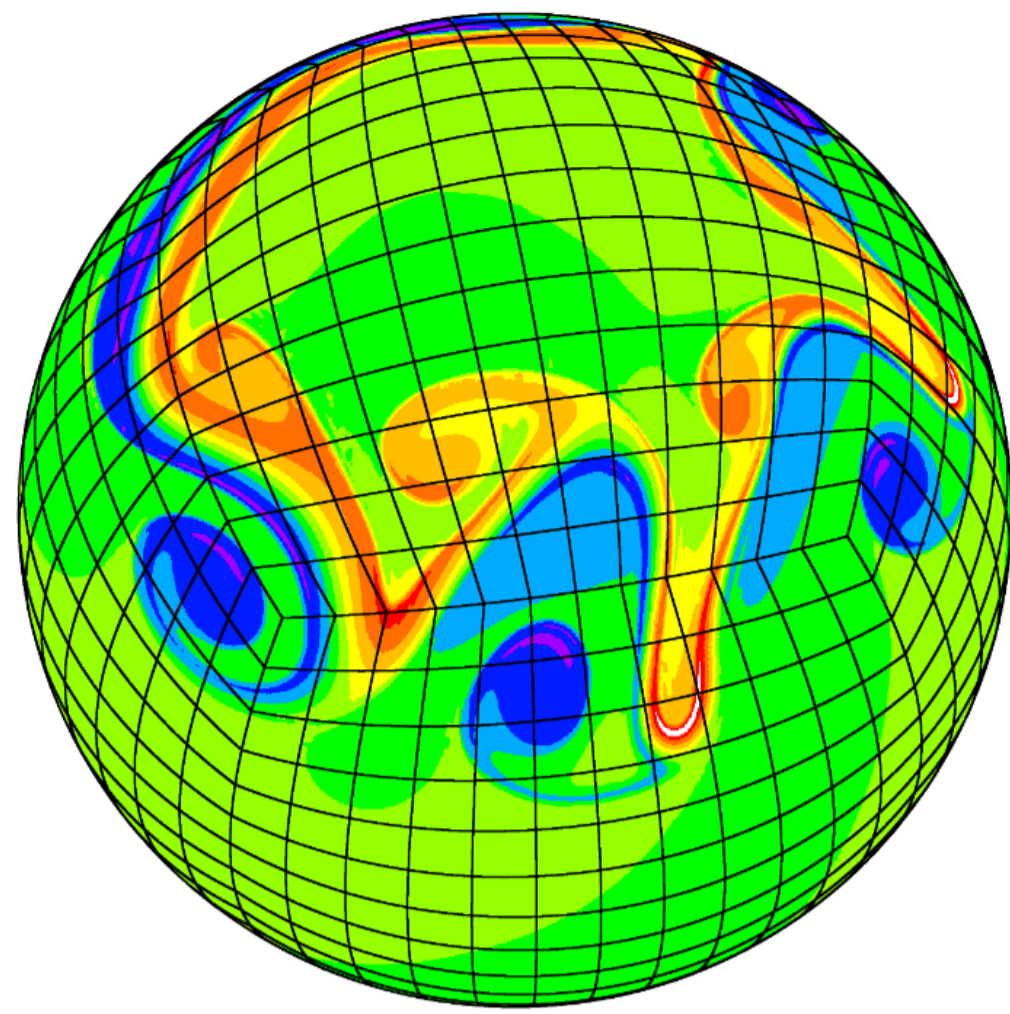
Taking into account a simplified meta-modeling approach (Margueron et al., 2018), the excluded range is estimated to encompass approximately 75% of the proposed nuclear EoSs.



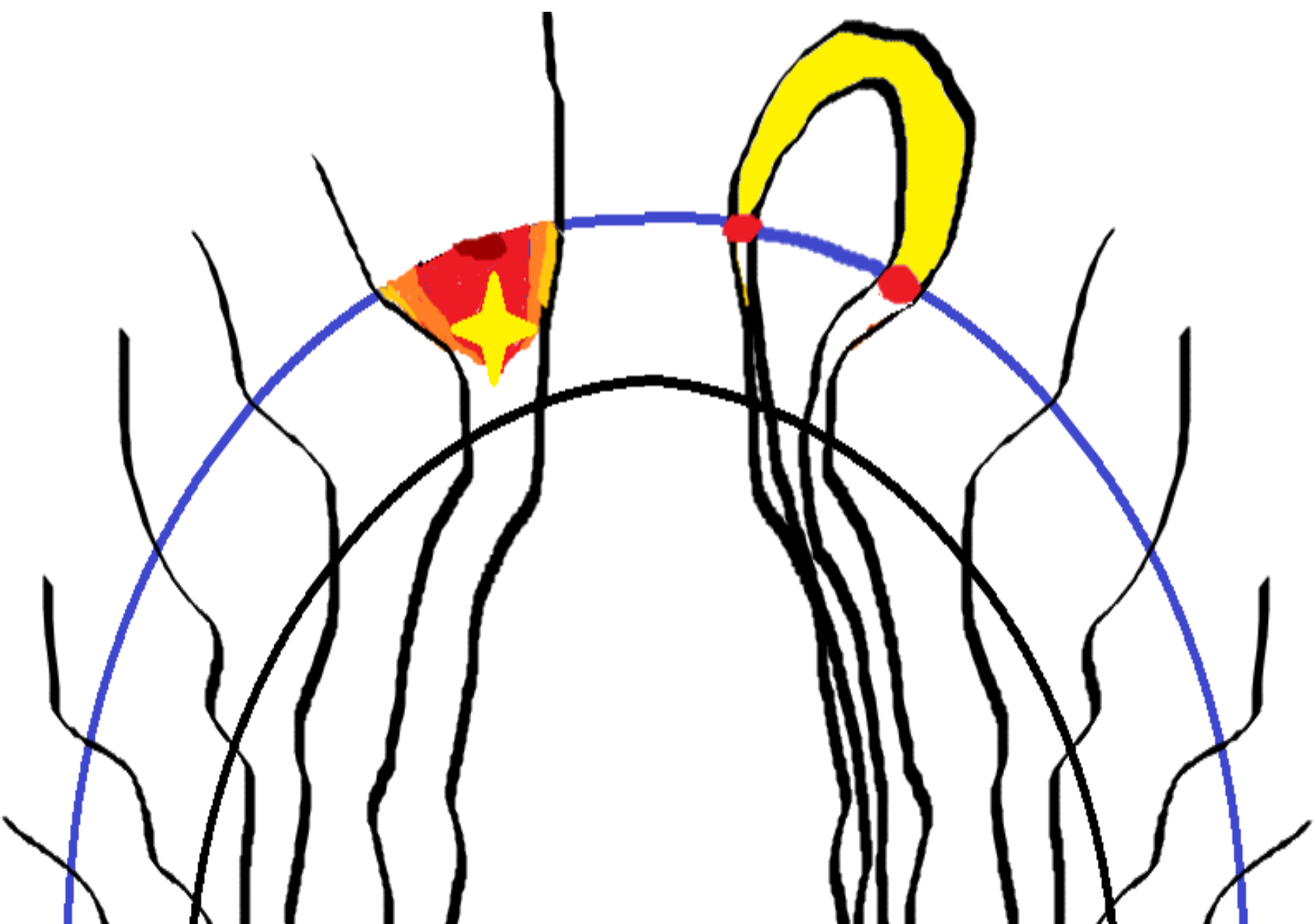
[Anzuini, Melatos, Dehman et al. 2021, MNRAS] } GM1A — with hyperons in  
 [Anzuini, Melatos, Dehman et al. 2022, MNRAS] } the core

[Marino, Dehman, Kowlakas, Rea et al. 2024, Nature Astronomy]





# Magnetic Field Evolution

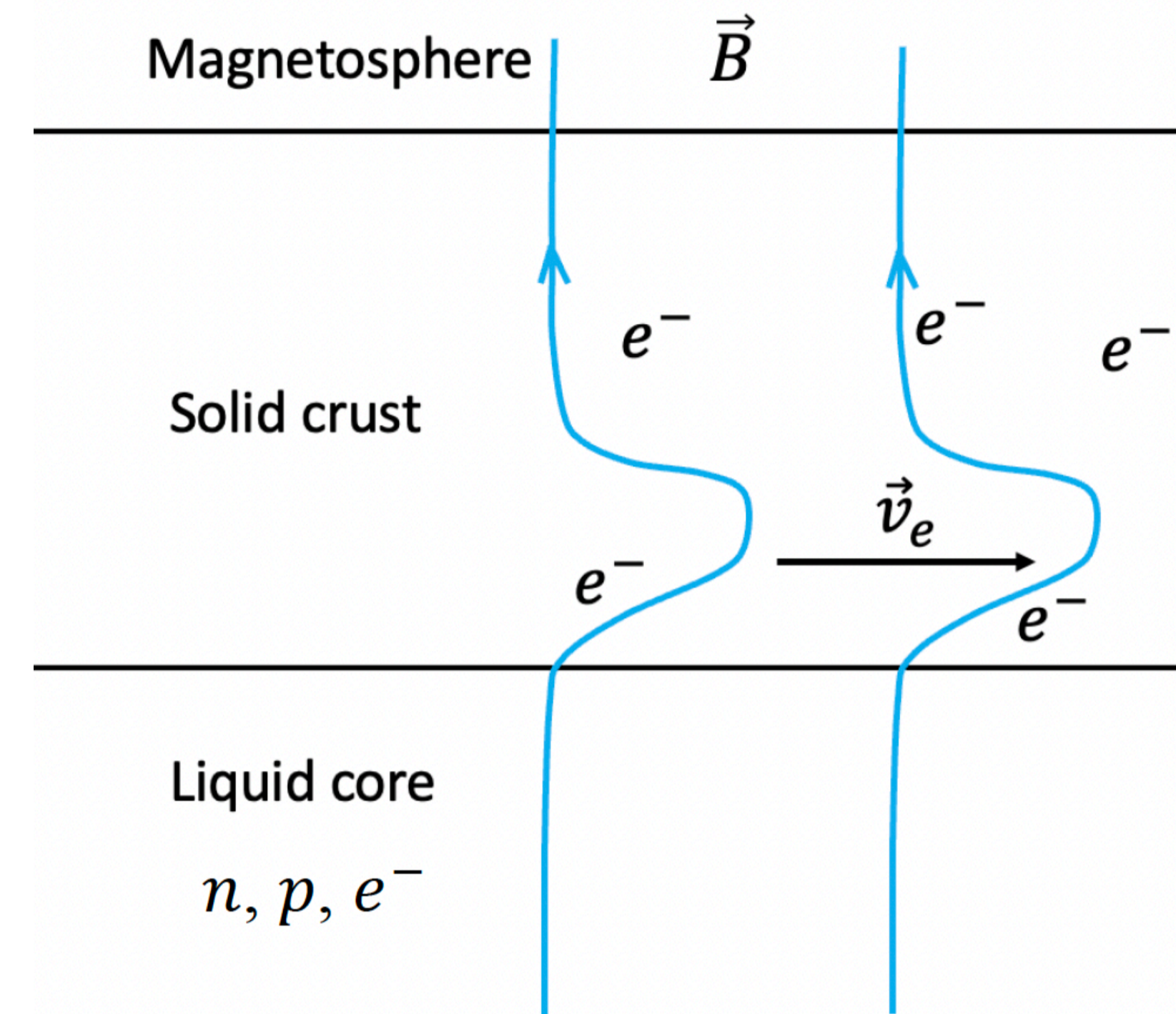


# Magnetic field evolution in the crust

- **Neutron star interior:** complex multi-fluid system.
- **Crust:** solidifies early; nuclei mobility is limited; conductivity governed by electrons.
- **Core:** remains a full multi-fluid on long timescales.
- **Limit:** eMHD used in the **crust of a neutron star**

$$\frac{\partial \mathbf{B}}{\partial t} = -\nabla \times \left[ \eta \nabla \times \mathbf{B} - \eta k_5 \mathbf{B} + f_h (\nabla \times \mathbf{B}) \times \mathbf{B} \right]$$

$$\left( \eta = \frac{c^2}{4\pi\sigma_e}; \quad k_5 = \frac{4\alpha\mu_5}{\hbar c}; \quad f_h = \frac{c}{4\pi en_e} \right)$$



**Ohmic term**  $\propto (\eta \nabla \times \mathbf{B})$ : the magnetic diffusivity is sensitive to temperature evolution and electron density (strong radial gradients).

**Chiral term**  $\propto (\eta k_5 \mathbf{B})$ : It redistributes magnetic energy among different magnetic spatial scales.

**Hall term**  $\propto (f_h (\nabla \times \mathbf{B}) \times \mathbf{B})$ : It naturally creates magnetic discontinuity and transfers energy between different scales.

**Perfect conductor B.C. at the crust-core interface (Meissner/type-I) and potential B.C. at the surface.**

$$k_5 = \frac{(\nabla \times \mathbf{B}) \cdot \mathbf{B}}{\frac{\mu_e^2}{8\pi\alpha^2\eta(\hbar c)}\Gamma_f + B^2} = \frac{(\nabla \times \mathbf{B}) \cdot \mathbf{B}}{\left(\frac{2\mu_e^2}{m_e^2 c^4}\right) \frac{B_{\text{QED}}^2}{3\pi} + B^2}$$

# MATINS the brand new 3D code

– Open Access: <https://github.com/ice-csic-astroexotic/MATINS>–

$$\frac{\partial \mathbf{B}}{\partial t} = -\nabla \times \left[ \eta \nabla \times (e^\nu \mathbf{B}) - \eta k_5 \mathbf{B} + f_h \nabla \times (e^\nu \mathbf{B}) \times \mathbf{B} \right] c_V(T) \frac{\partial (T e^\nu)}{\partial t} = \vec{\nabla} \cdot (e^\nu \hat{\mathbf{k}} \cdot \vec{\nabla} (e^\nu T)) + e^{2\nu} (Q_J - Q_\nu)$$

[Dehman, Viganò, Pons & Rea 2023, MNRAS \(DOI: \[10.1093/mnras/stac2761\]\(https://doi.org/10.1093/mnras/stac2761\)\)](#): Cubed-sphere grid + Magnetic formalism

[Dehman, Viganò, Ascenzi, Pons & Rea 2023, MNRAS \(DOI: \[10.1093/mnras/stad1773\]\(https://doi.org/10.1093/mnras/stad1773\)\)](#): First 3D magneto-thermal simulation

[Ascenzi, Viganò, Dehman, Pons & Rea, Perna 2024, MNRAS \(DOI: \[10.1093/mnras/stae1749\]\(https://doi.org/10.1093/mnras/stae1749\)\)](#): Thermal formalism

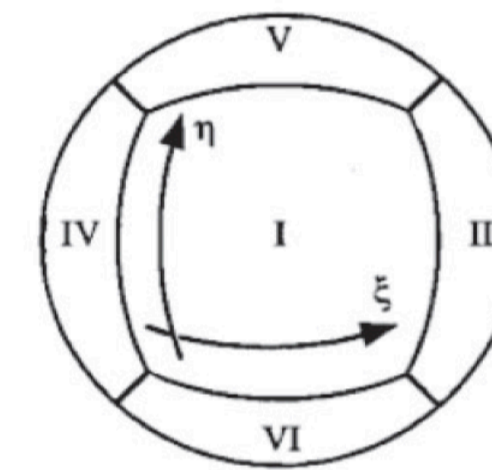
[Dehman & Pons 2025, PRR \(DOI: \[10.1103/rhv5-nd4v\]\(https://doi.org/10.1103/rhv5-nd4v\)\)](#): Chiral magnetic effect

What's better than 2D (Viganò et al. 2021):

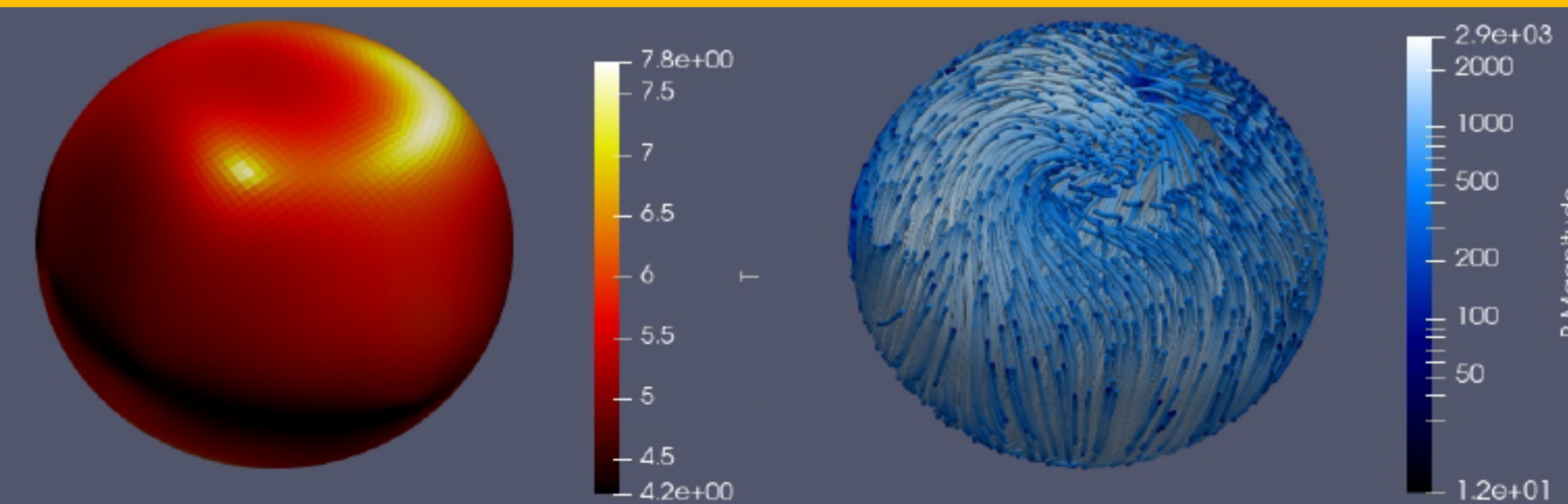
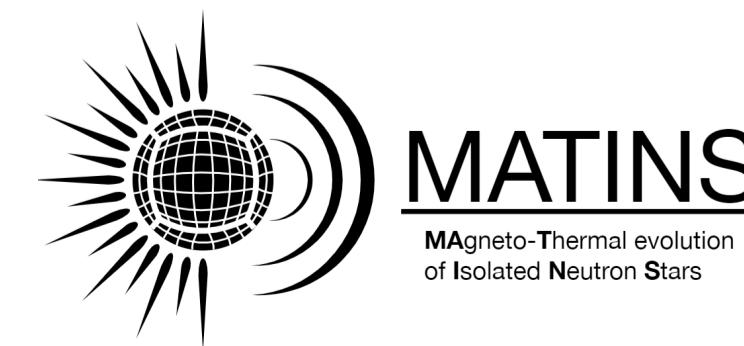
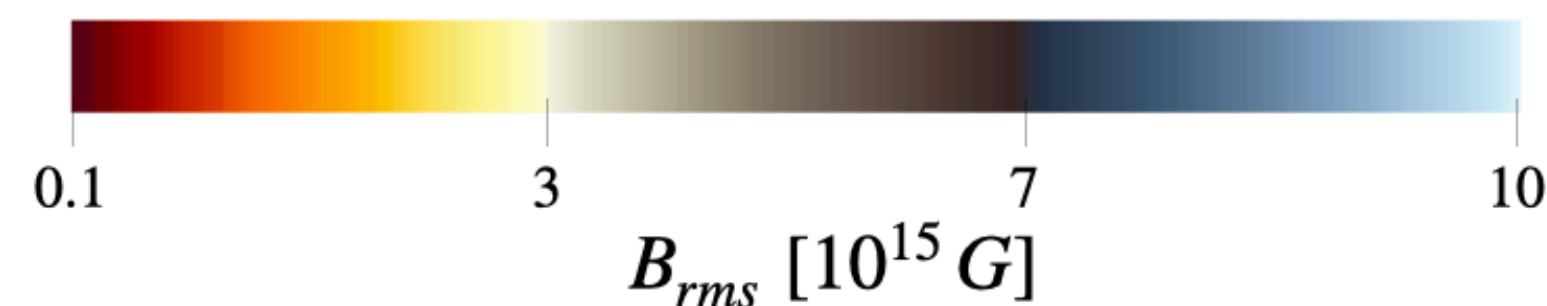
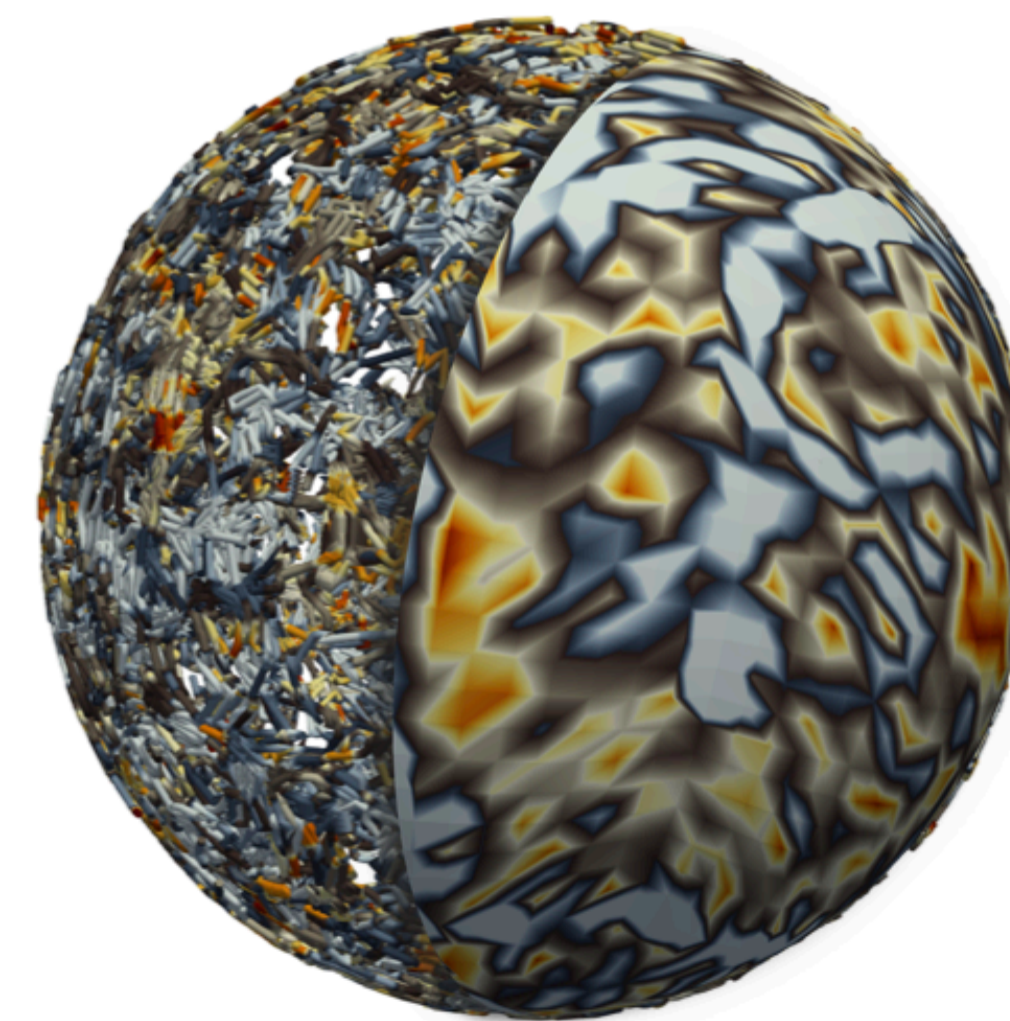
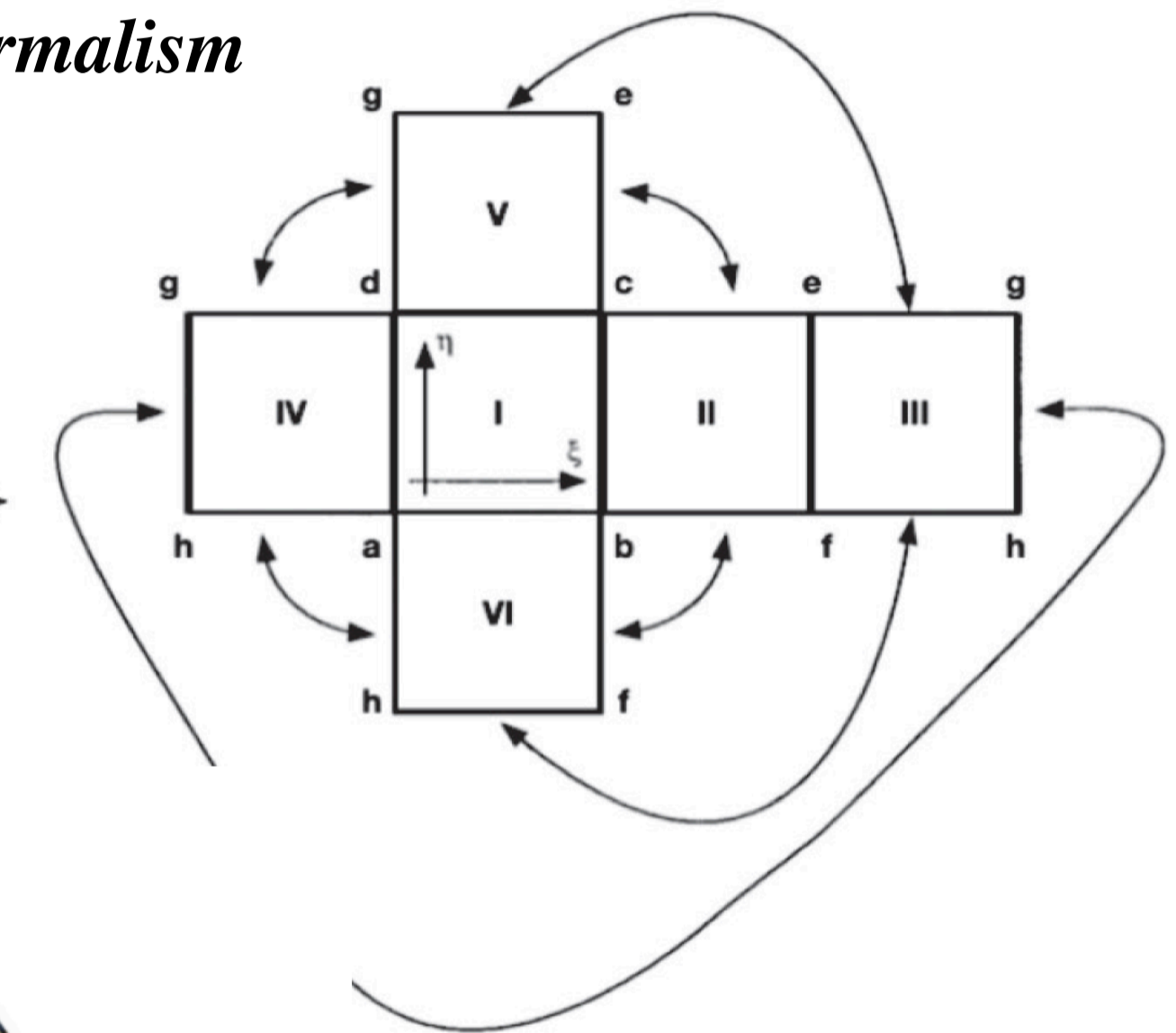
- Simulation of 3D magnetic modes, hotspots, and light curves
- Better documentation, **use of novel coordinates (cubed-sphere)**
- Optimization and use of OpenMP

Advance obtained:

- **Realistic 3D evolution and topology, appearance of hotspots**
- **State-of-the-art microphysics, various masses and EOSs, with realistic structure obtained by solving the TOV equation.**
- **Numerical scheme to better capture non-linear dynamics**
- **General relativistic correction**
- **State of art envelope model**
- **Flexibility in implementing new physics**



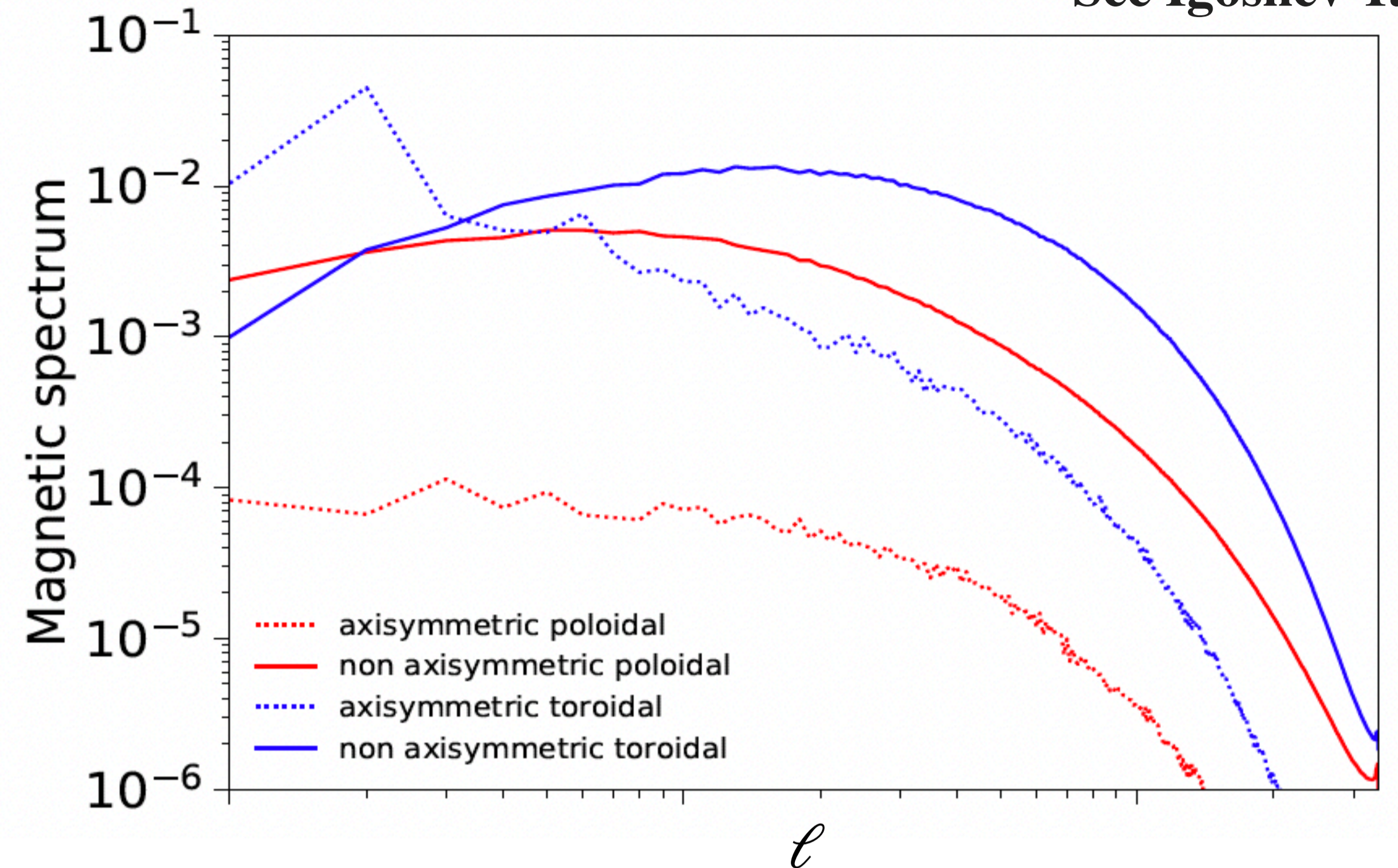
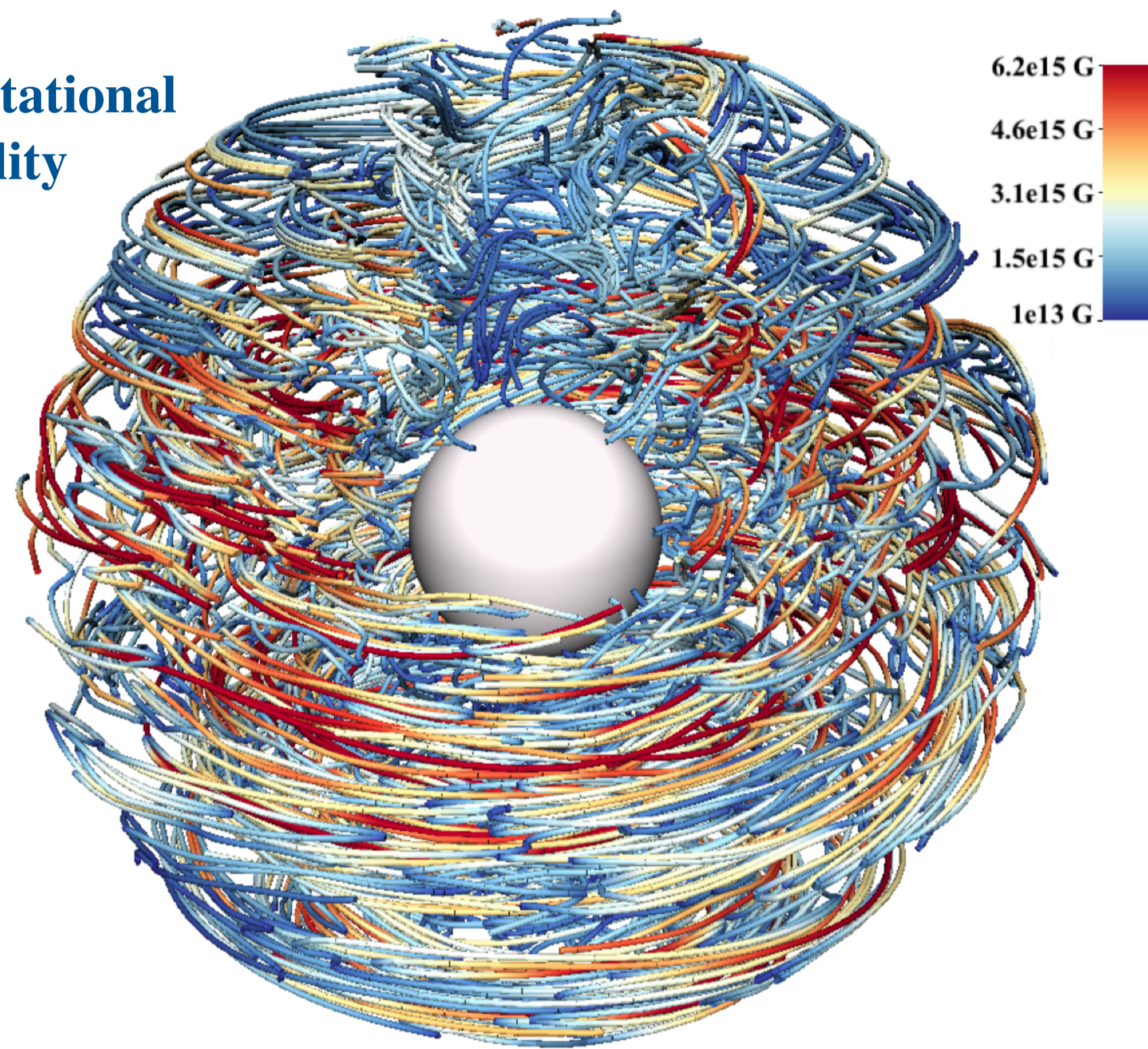
**cubed sphere**



# Magnetic field at birth: Magnetic spectrum after core-collapse

See Igoshev Talk

Magneto-rotational instability



Magnetic energy is distributed across a broad range of scales.

Toroidal axisymmetric quadrupole and non-axisymmetric components dominate.

Dipolar field accounts for less than 5% of the total magnetic energy ( $\approx 10^{12}$  G).

From post-collapse to neutron star phase, plenty of MHD timescales to approach an equilibrium, with dynamo still going on and at the same time dissipating the smallest scales.

**But how does a strong dipole of  $10^{14}$  G form in magnetars, leading to their long spin periods?**

[Reboul-Salze et al. 2022]

[Dehman et al. 2023c]

[Barrère et al. 2025]

[Igoshev et al. 2025]

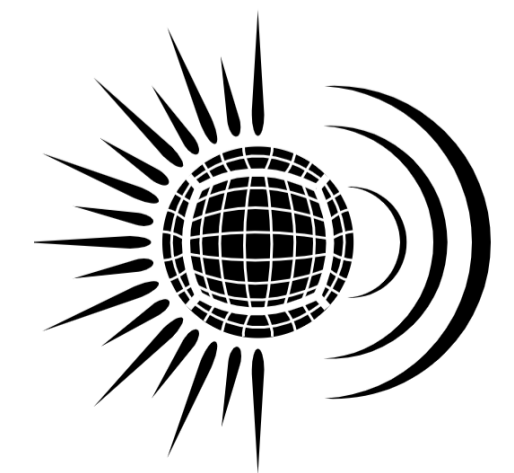
Magneto-rotational instability

Taylor-Spruit dynamo

Candidates to explain CCOs, low field magnetars



Weak dipolar component (order of  $10^{12}$  G)



**MATINS**  
MAGneto-Thermal evolution of Isolated Neutron Stars

# Hall-driven inverse cascade in neutron star crusts

## Initial field:

Helical magnetic field.

Random initial field peaking at  $\ell_0 \sim 100$ .

Causal spectrum as used in the cosmological context.

**Correct aspect ratio of the NS crust.**

## Inverse Cascade occurs!

Energy transferred from small to large-scale multipoles.

**Not observed in previous neutron star simulation studies.**

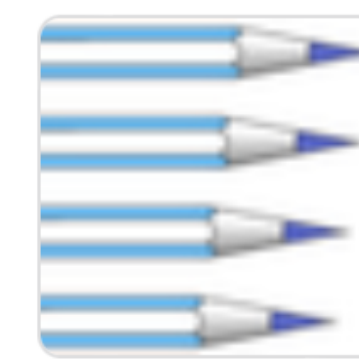
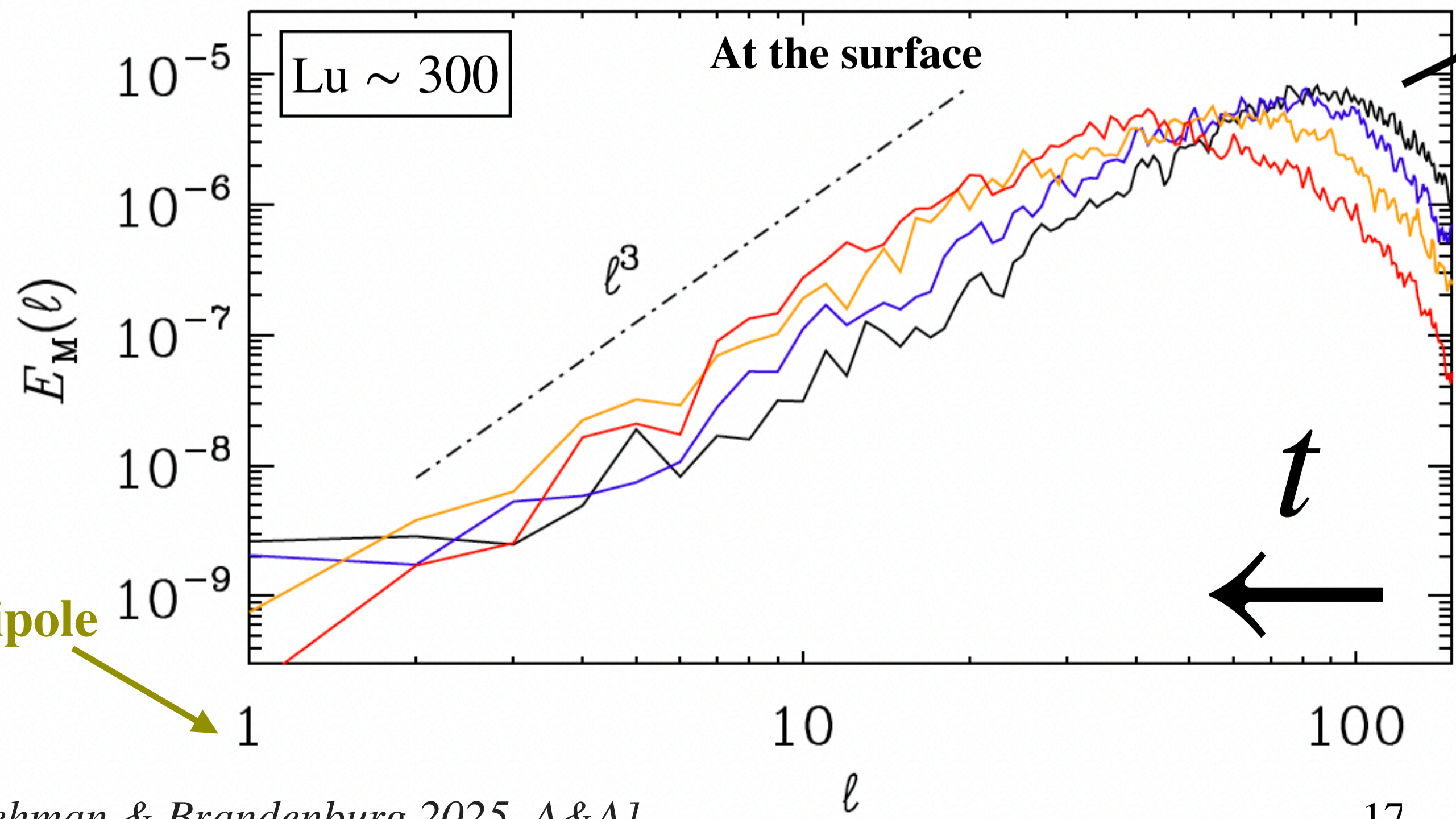
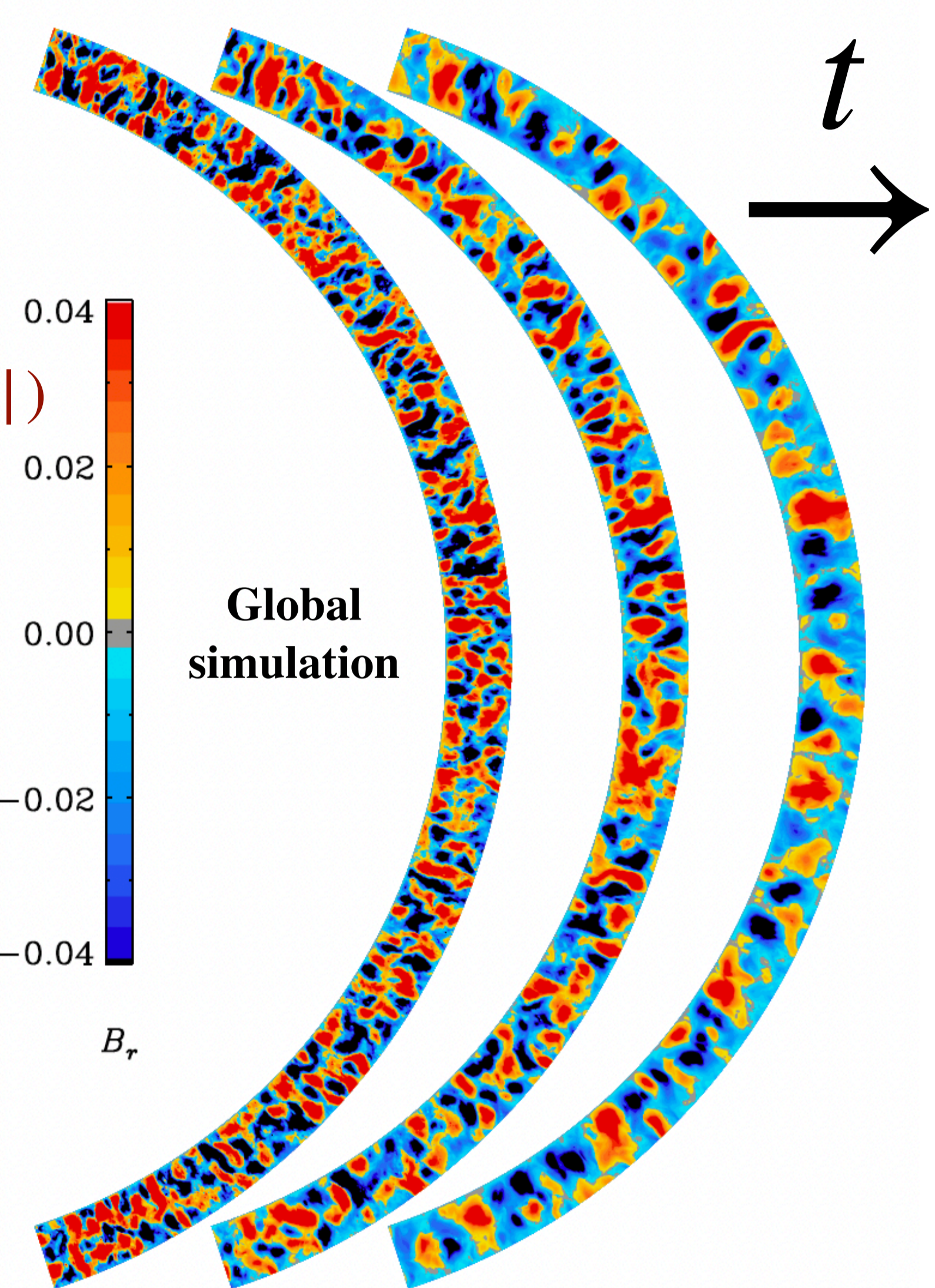
Extreme aspect ratio (1:30)—thin crust—limits the inverse cascade.

Maximally helical  
(e.g., positive helicity):

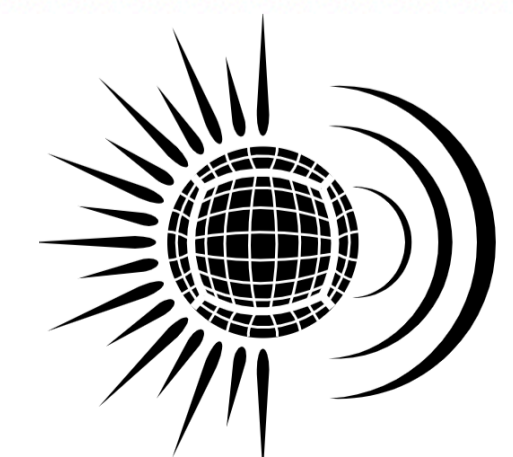
$$k = p + q$$

$$\begin{aligned} k |H_M(k)| / 2E_M(k) &\leq 1 \\ H_M &= 2E_M(k)/k \end{aligned}$$

$$|k| \leq \max(|p|, |q|)$$



Pencil Code

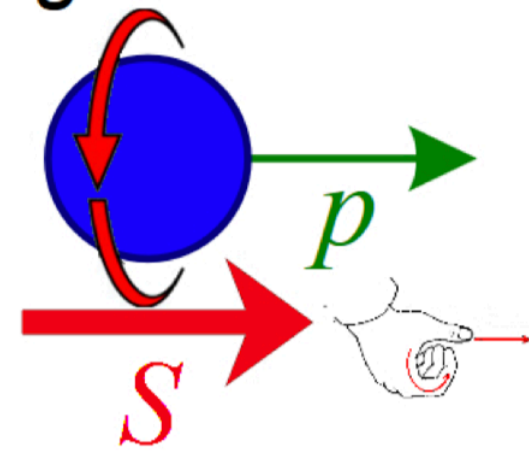


**MATINS**

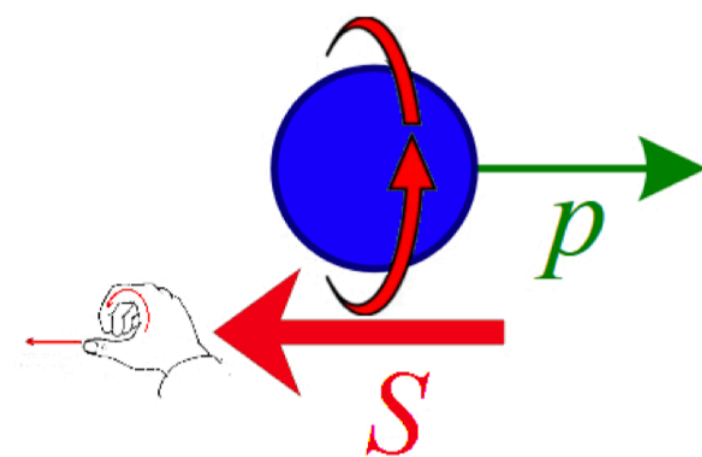
MAGneto-Thermal evolution  
of Isolated Neutron Stars

# Chiral Anomaly

Right-handed



Left-handed



A particle is moving with momentum  $p$  represented by the green arrow.

## — Particle Chirality —

The chirality of a particle is the projection of the spin along the direction of movement:

- right-handed if it is parallel to the movement;
- left-handed otherwise.

## — Magnetic Helicity —

- Pure poloidal & toroidal components are unstable
- Both components are necessary for the stability (linked structures)
- Magnetic helicity quantify the topological stability

$$\frac{\partial (A \cdot B)}{\partial t} = -2cE \cdot B - c\nabla \cdot (E \times A)$$

## — Chiral Anomaly —

- Changes in magnetic helicity create or destroy chiral asymmetry (vice versa).
- Chiral electric current induced along field lines

$$\frac{\partial n_5}{\partial t} = \frac{2\alpha}{\pi\hbar} E \cdot B - n_5 \Gamma_f$$

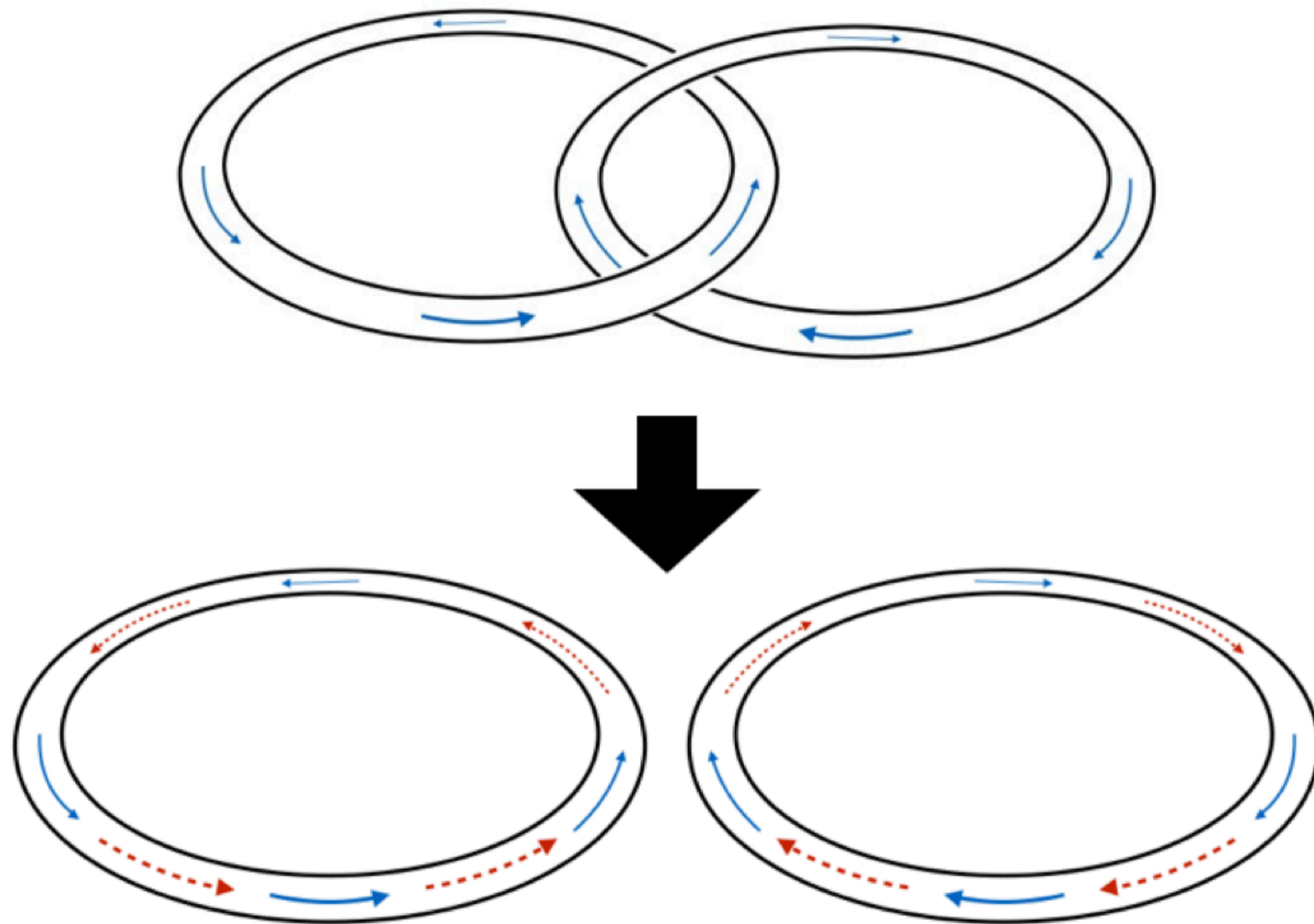
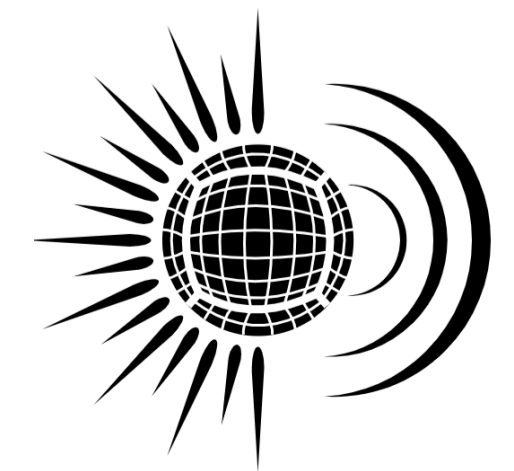
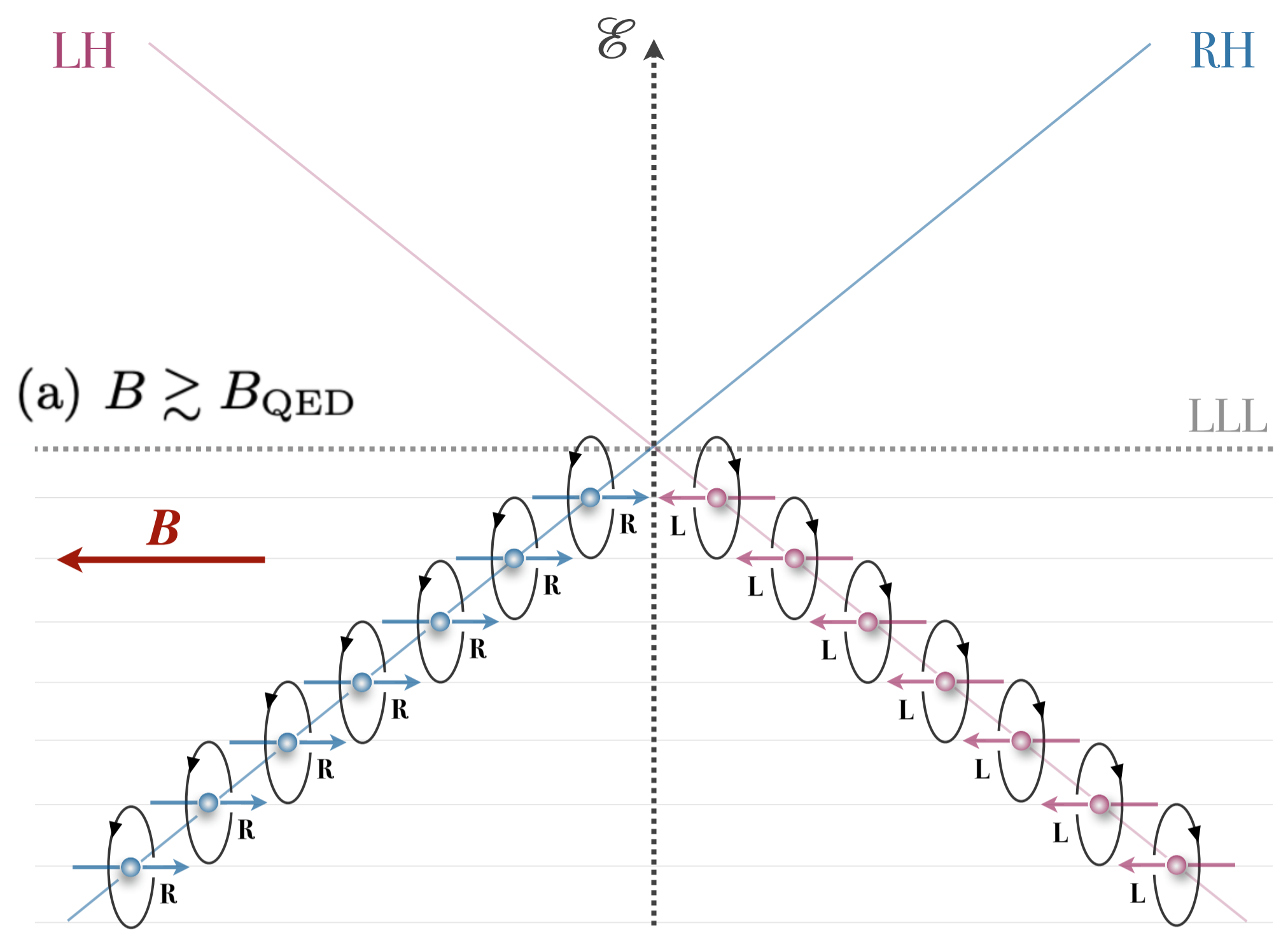
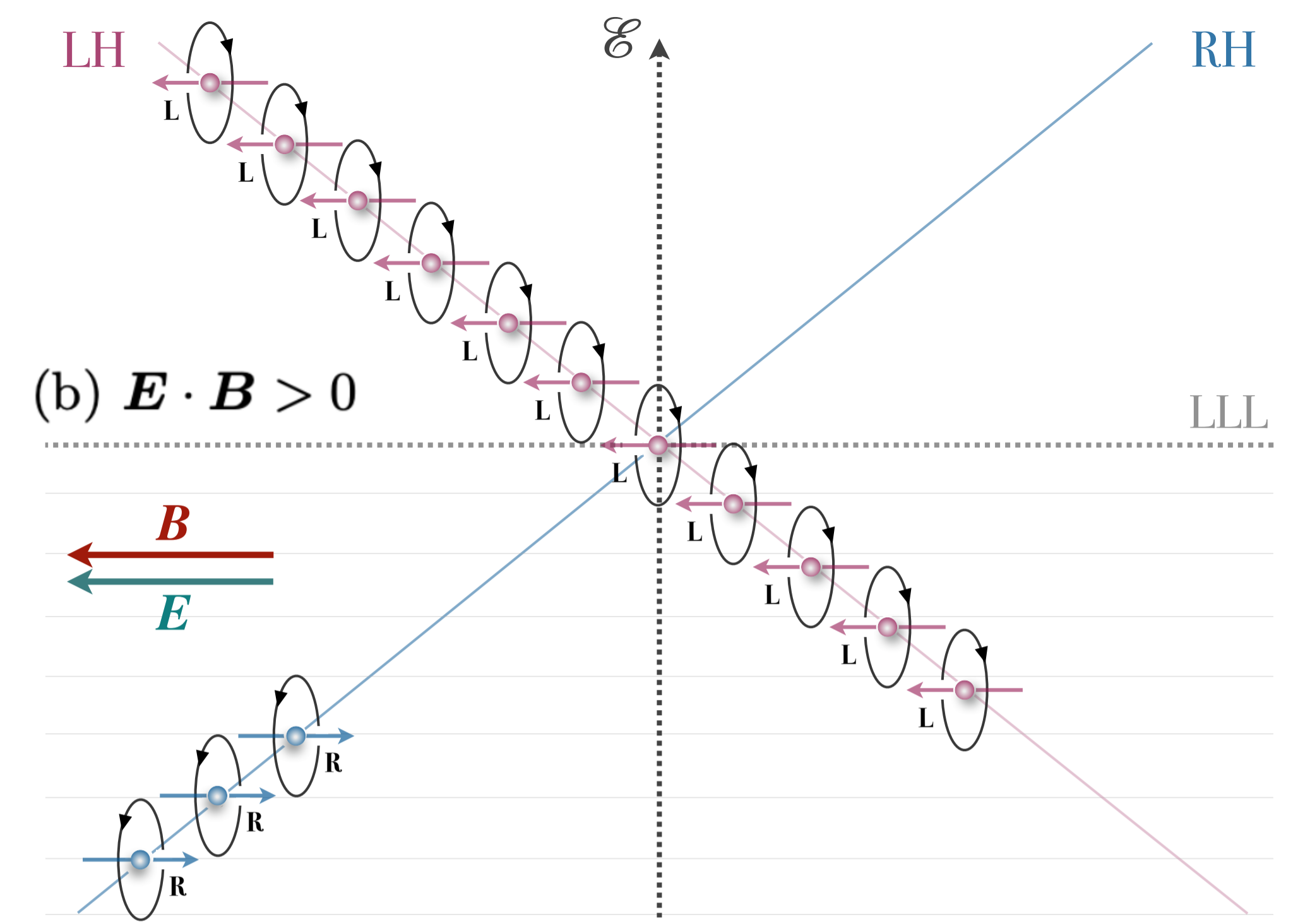
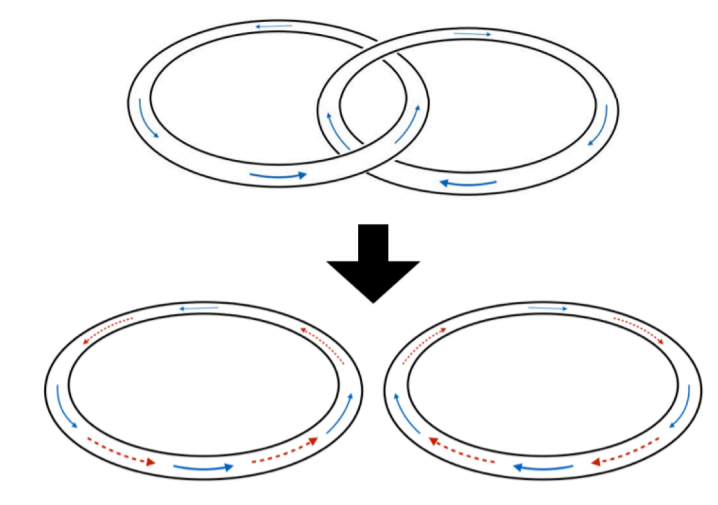
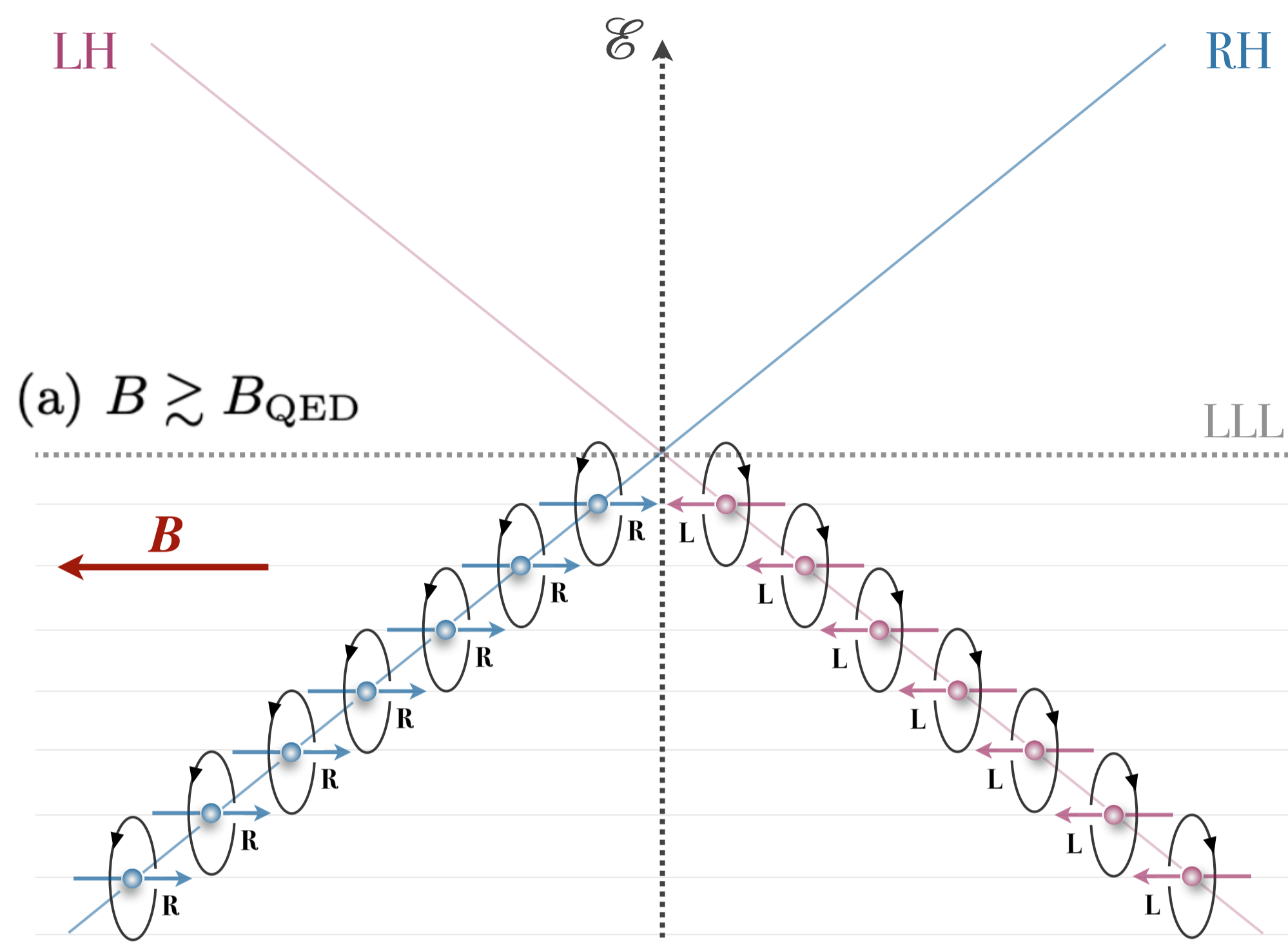
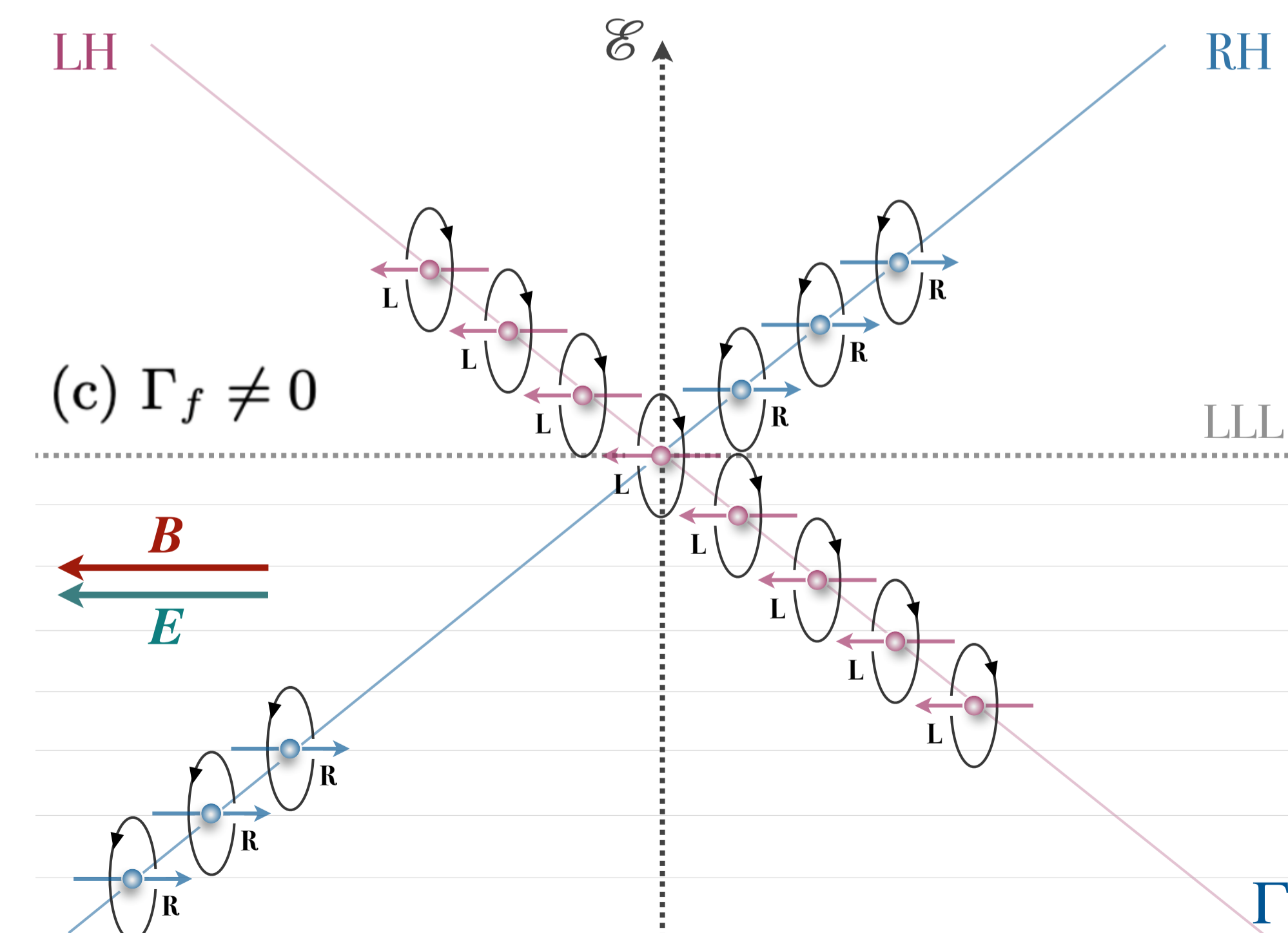
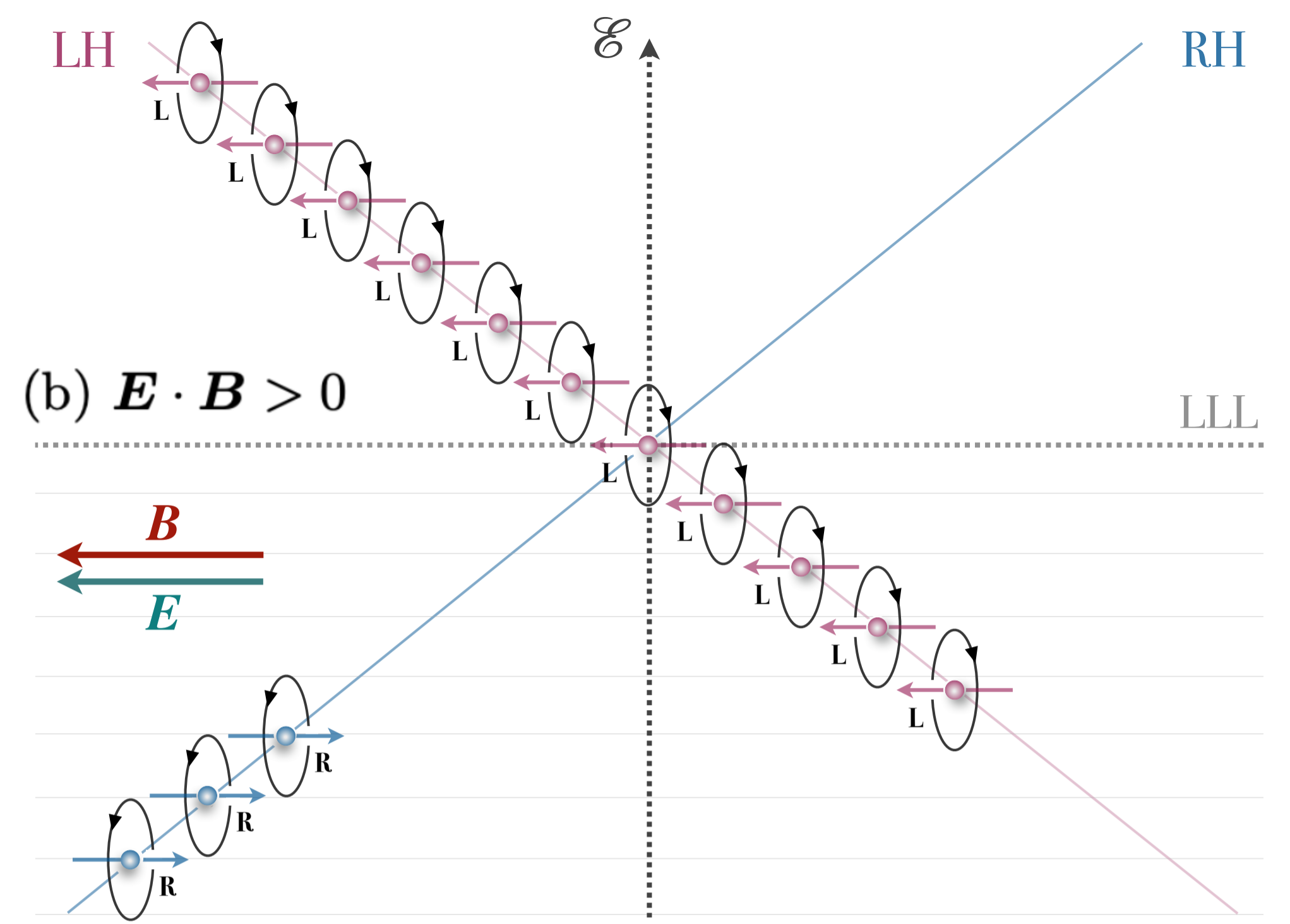
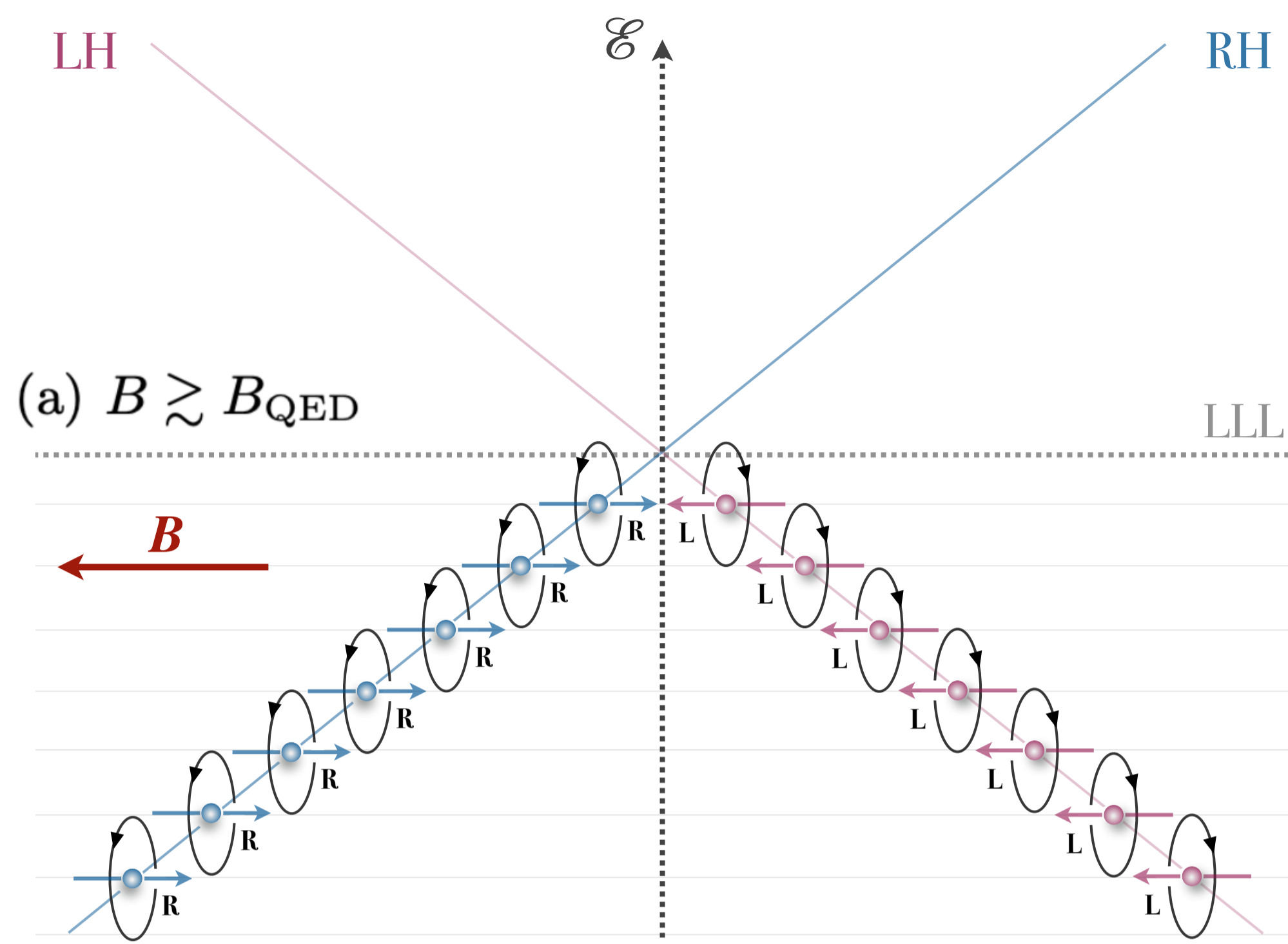


Image credit: Y. Hirono



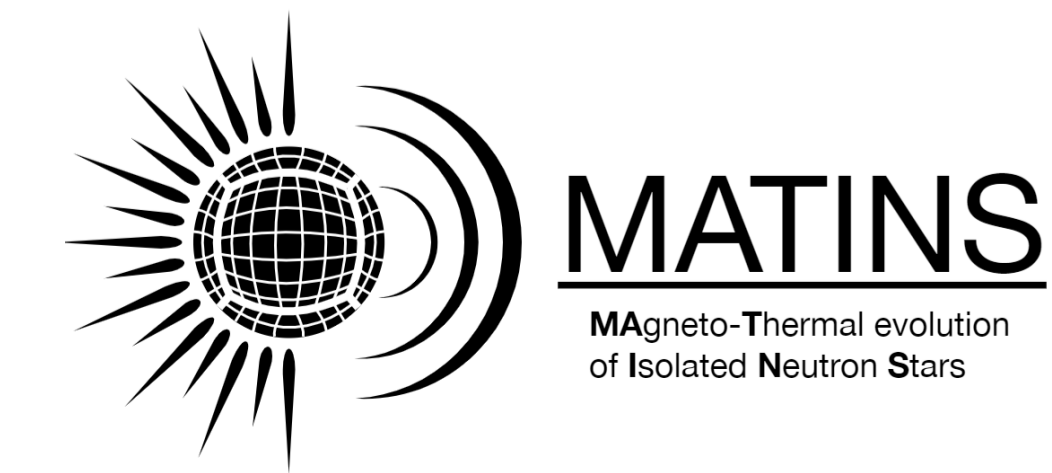


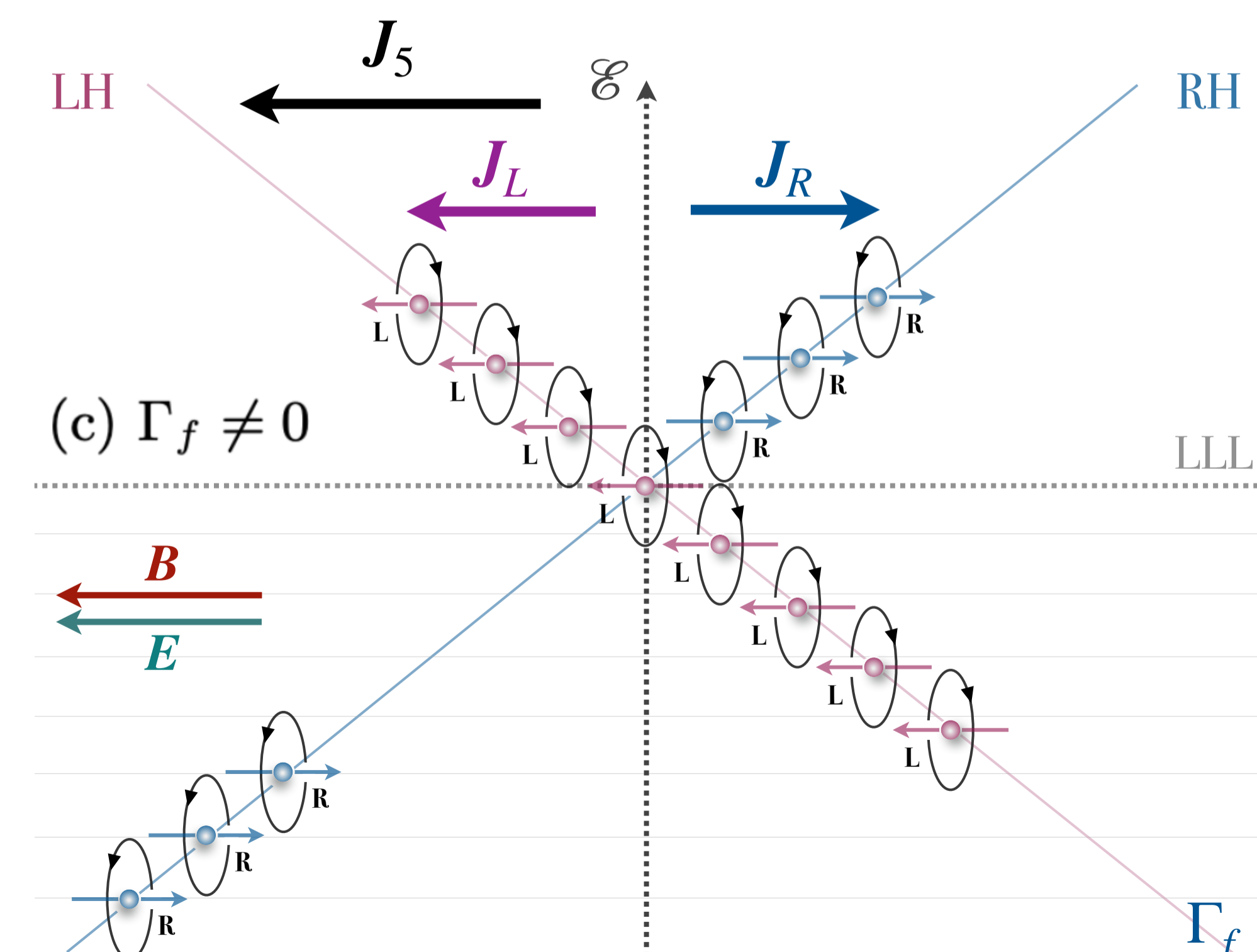
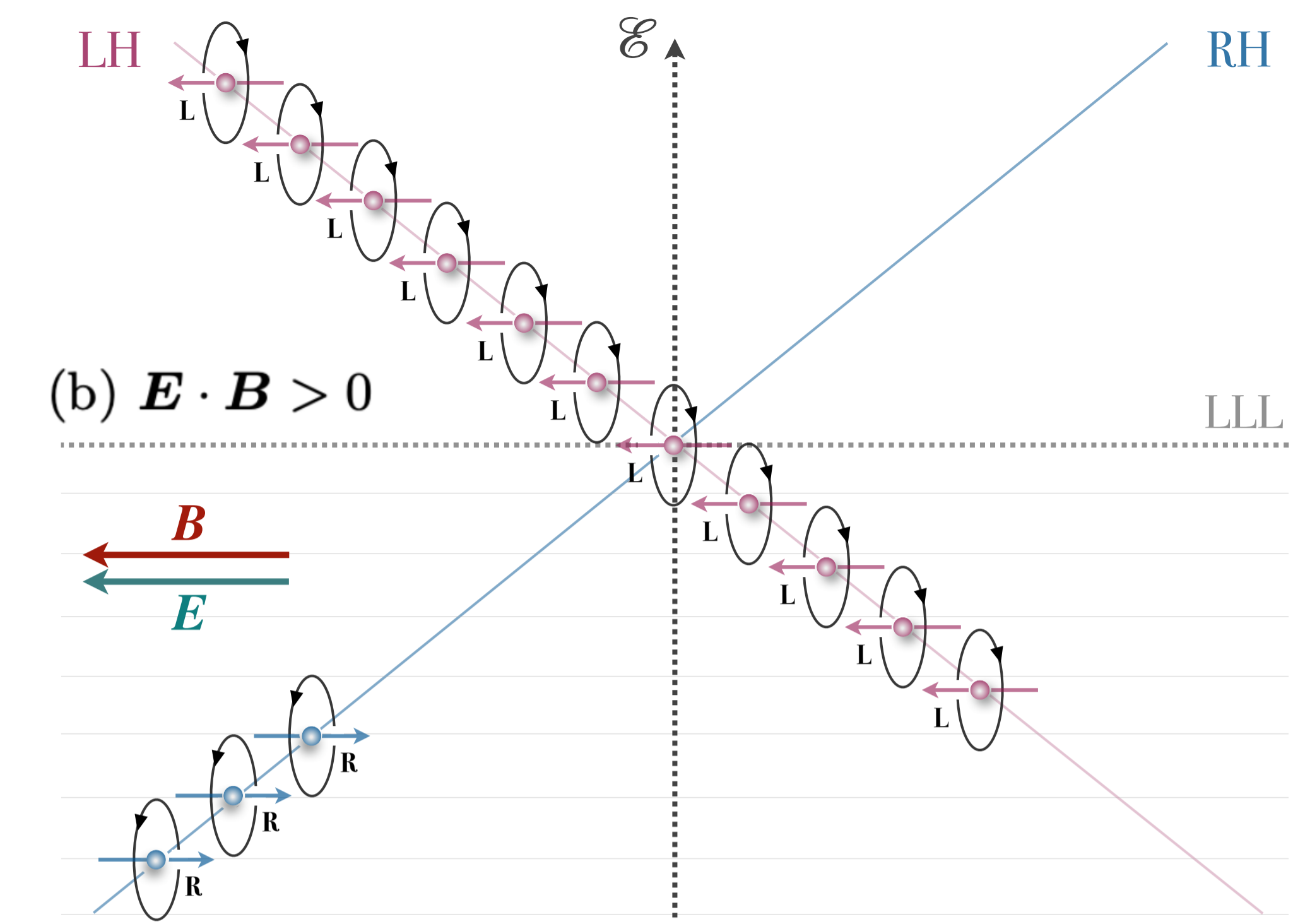
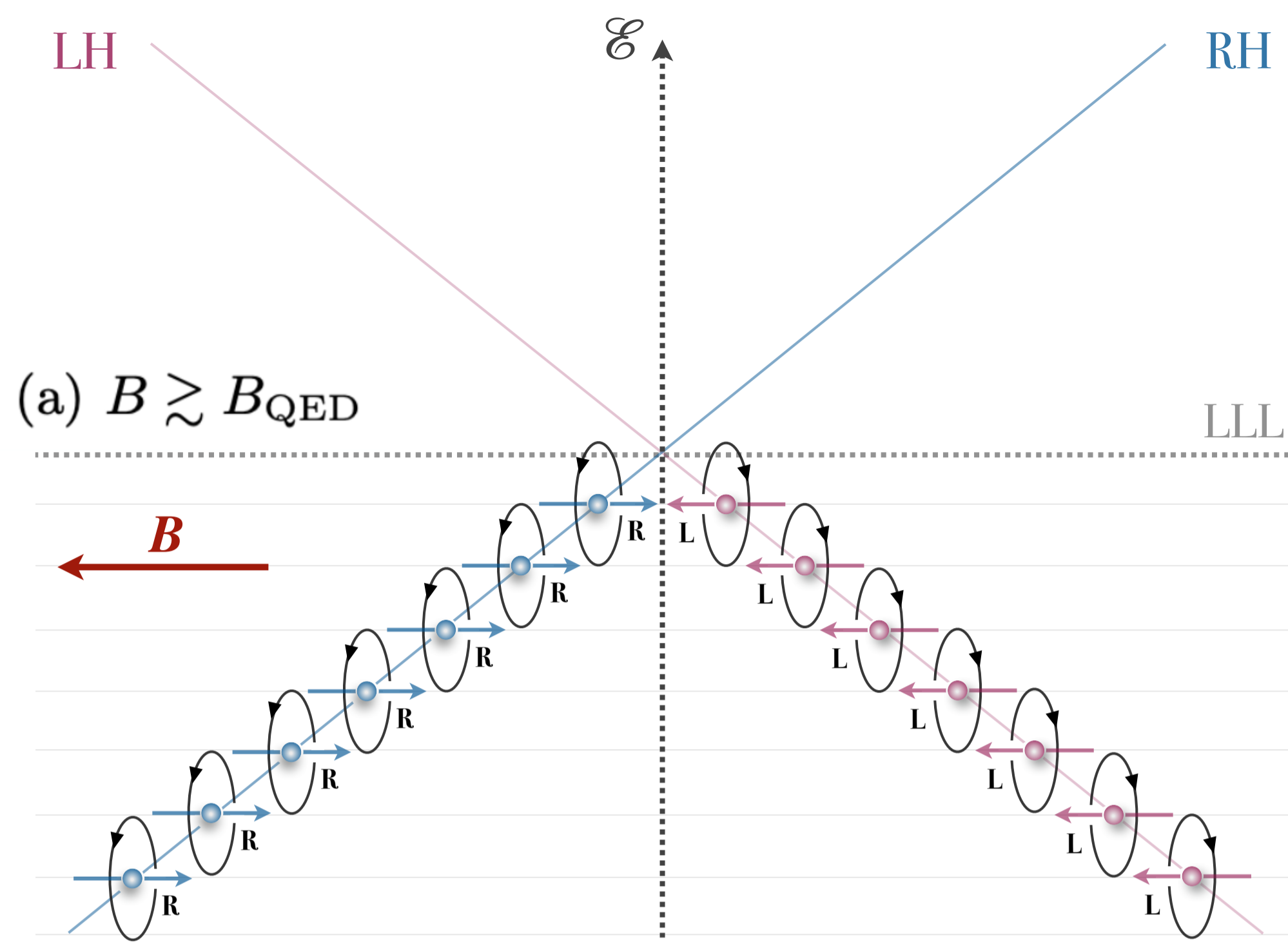




$$\Gamma_f = \left( \frac{m_e}{\mu_e} \right)^2 \nu_{\text{coll}} = \frac{4\alpha}{3\pi\sigma_e} \frac{m_e^2 c^4}{\hbar^2}$$

[Dehman 2026, arXiv: 2605.08068]





$$J_5 = J_R + J_L = \frac{\alpha}{\pi \hbar} \mathbf{B} (\mu_R - \mu_L) = \frac{\alpha \mu_5}{\pi \hbar} \mathbf{B}$$

$$|\mu_5| \approx 10^{-12} \dots 10^{-11} \text{ MeV} \ll \mu_e = 10 \dots 100 \text{ MeV}$$

$$\mathbf{J} = \frac{c}{4\pi} (\nabla \times \mathbf{B}) = \sigma_e \mathbf{E} + \mathbf{J}_5$$

$$\frac{\partial \mathbf{B}}{\partial t} = -\nabla \times [\eta \nabla \times \mathbf{B} - \eta k_5 \mathbf{B}] + f_h (\nabla \times \mathbf{B}) \times \mathbf{B}$$

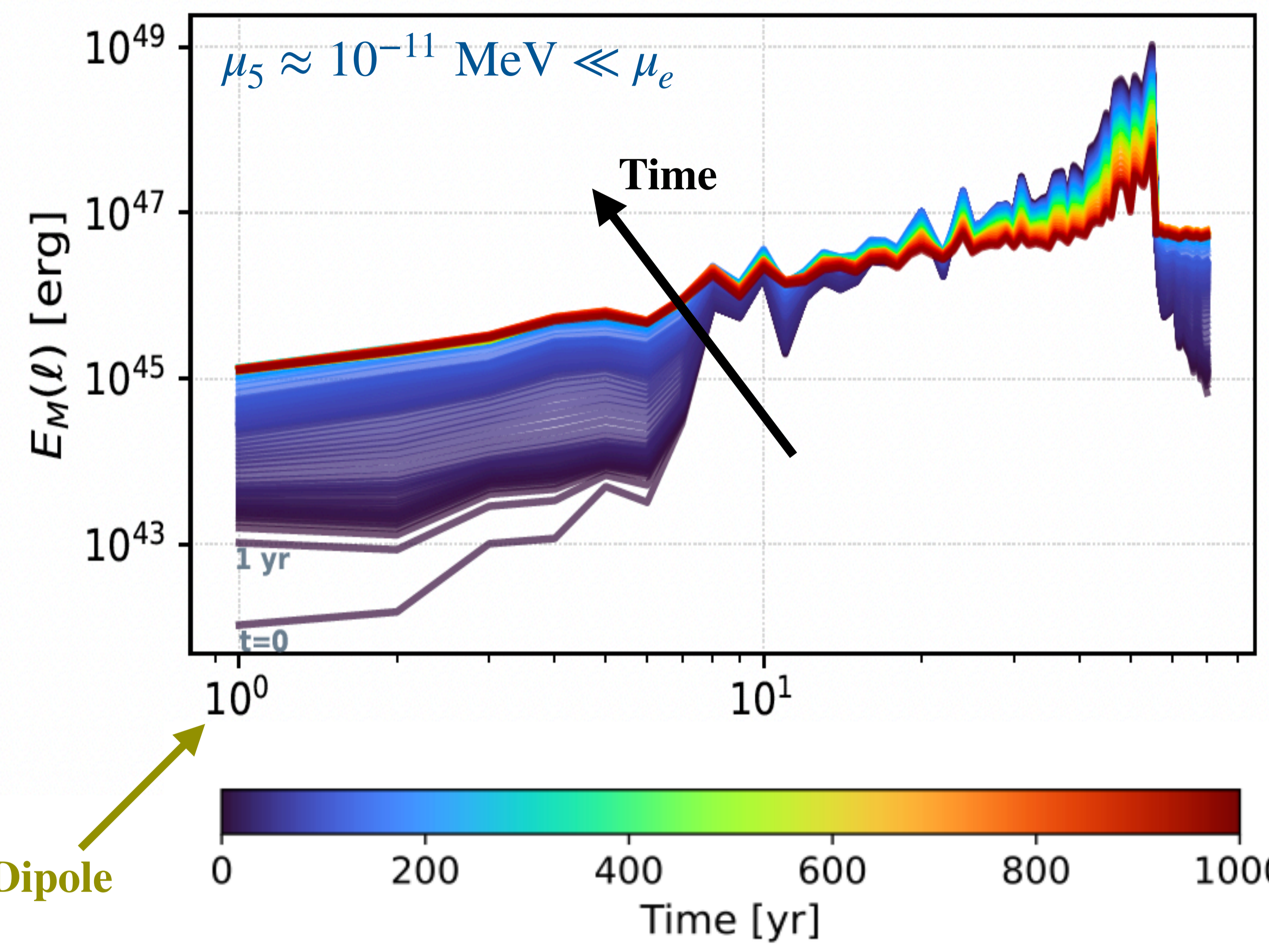
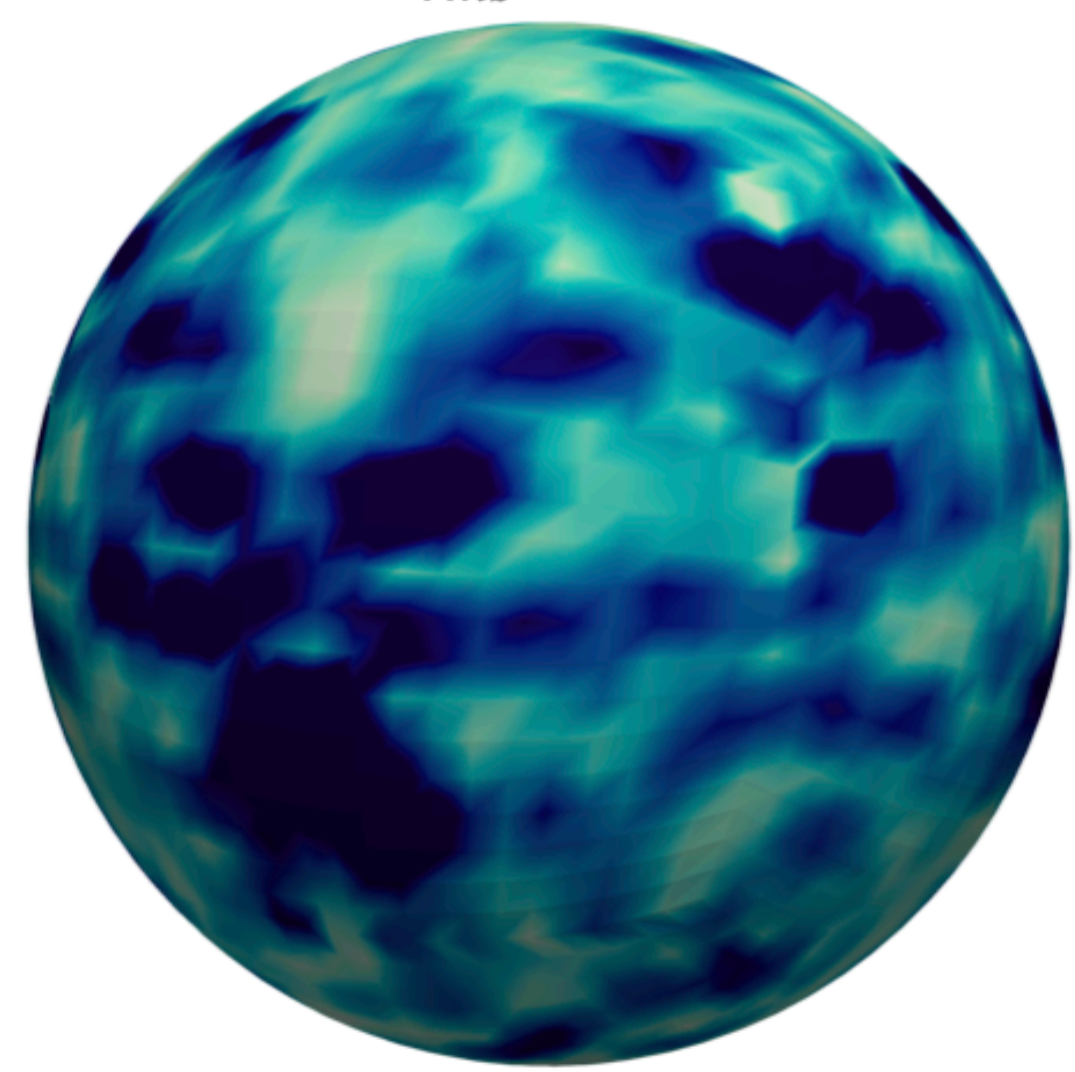
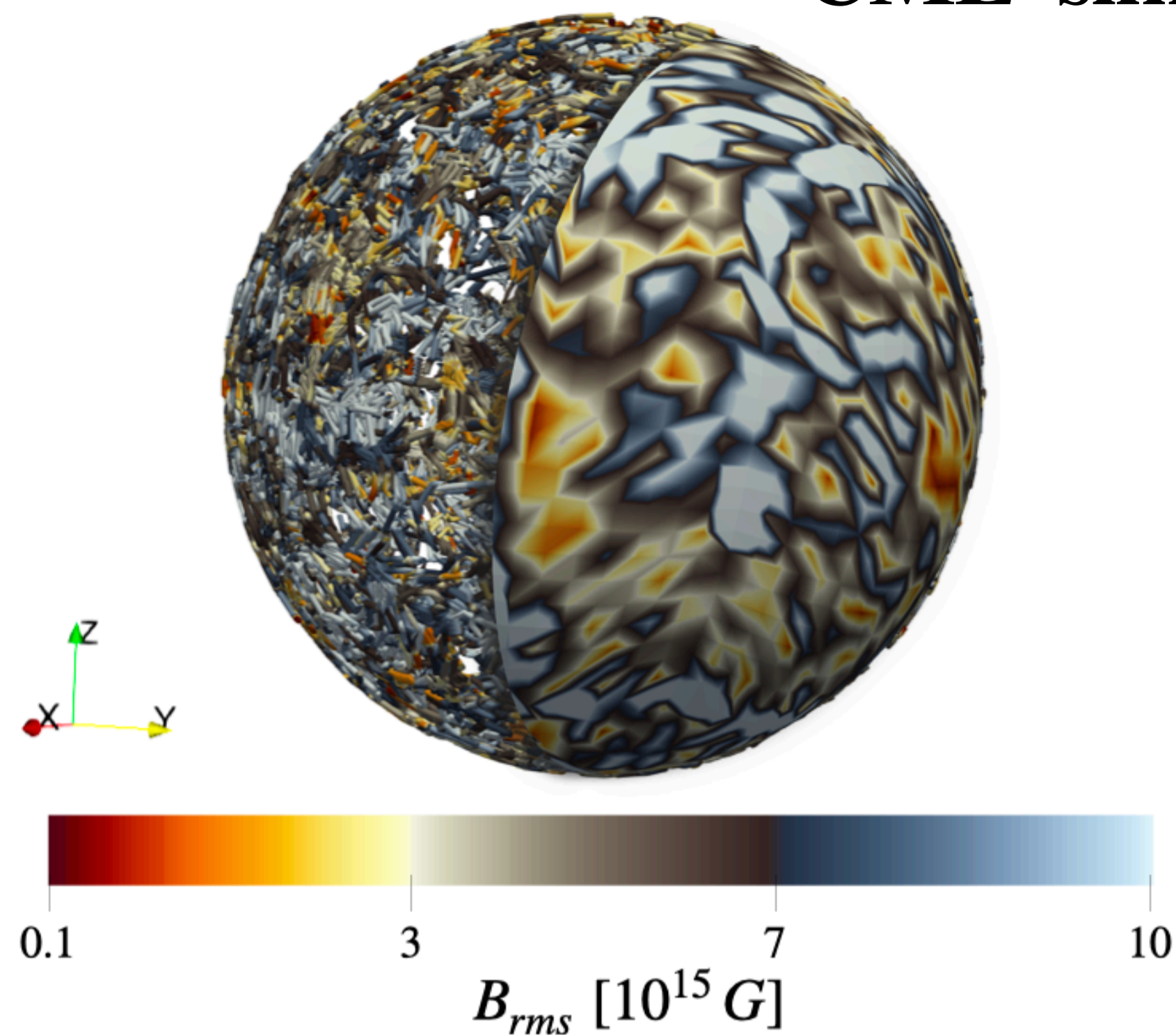
[Dehman & Pons 2025, PRR]

$$\Gamma_f = \left( \frac{m_e}{\mu_e} \right)^2 \nu_{\text{coll}} = \frac{4\alpha}{3\pi\sigma_e} \frac{m_e^2 c^4}{\hbar^2}$$

[Dehman 2026, arXiv: 2605.08068]



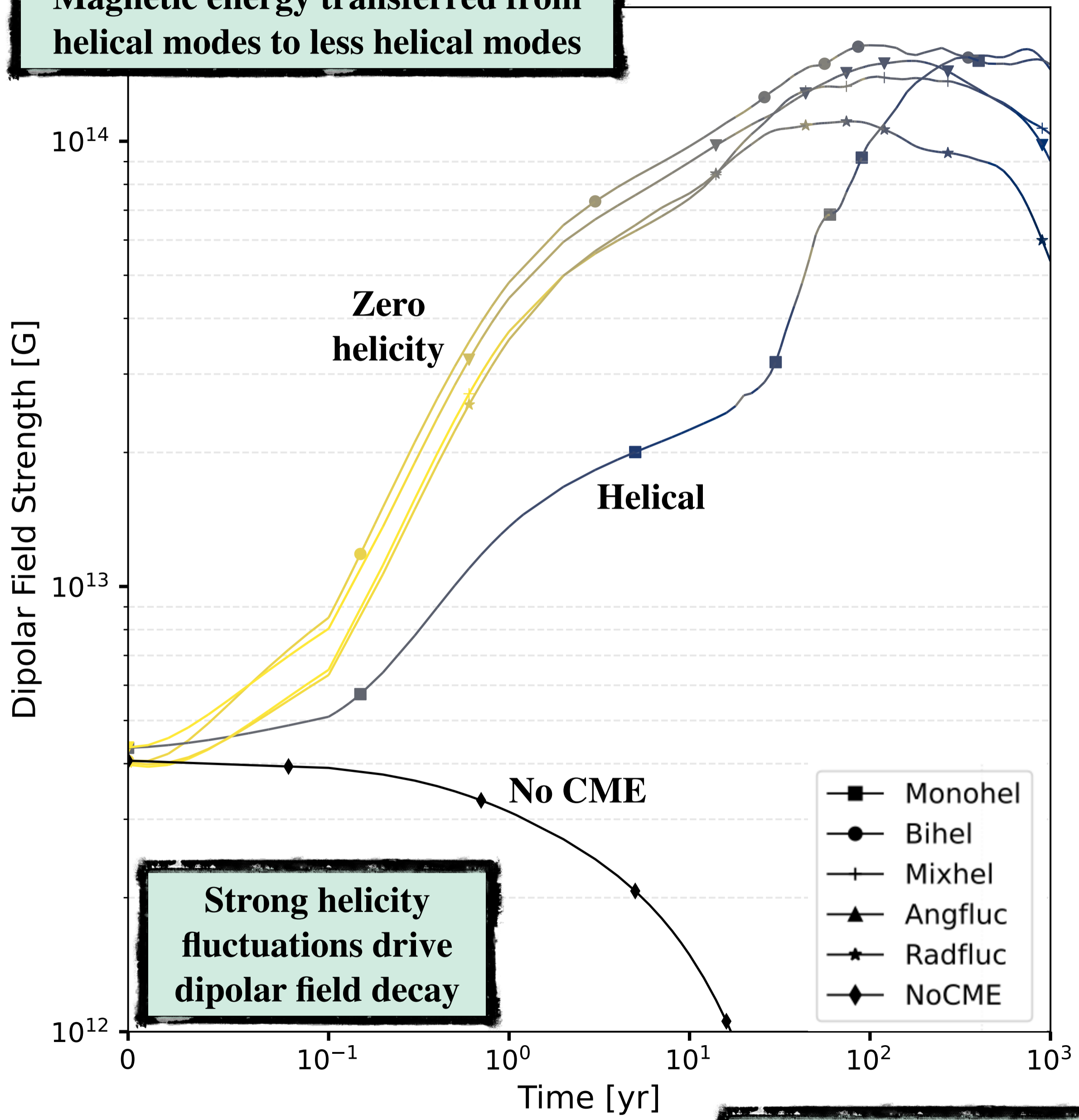
# CME simulations — net magnetic helicity



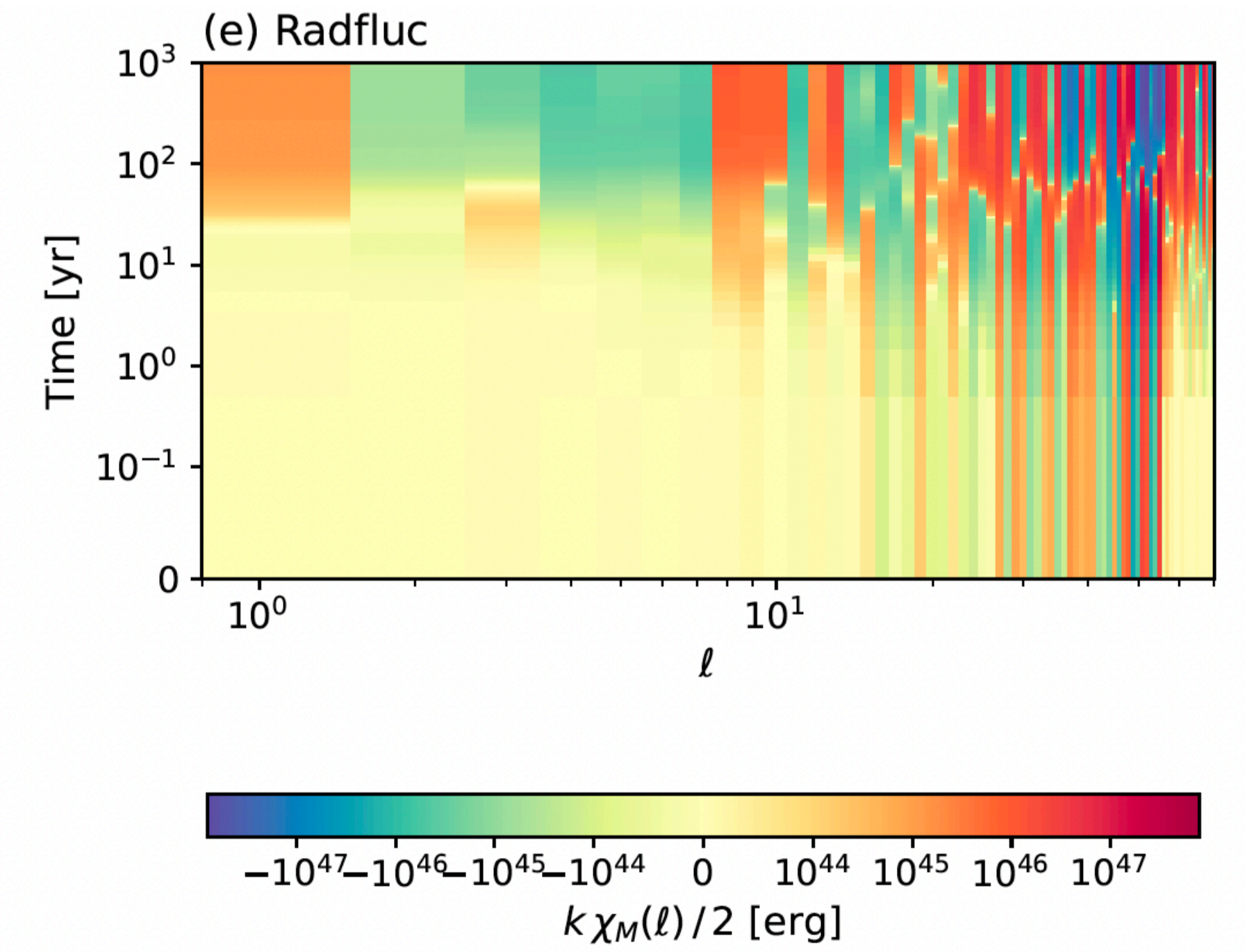
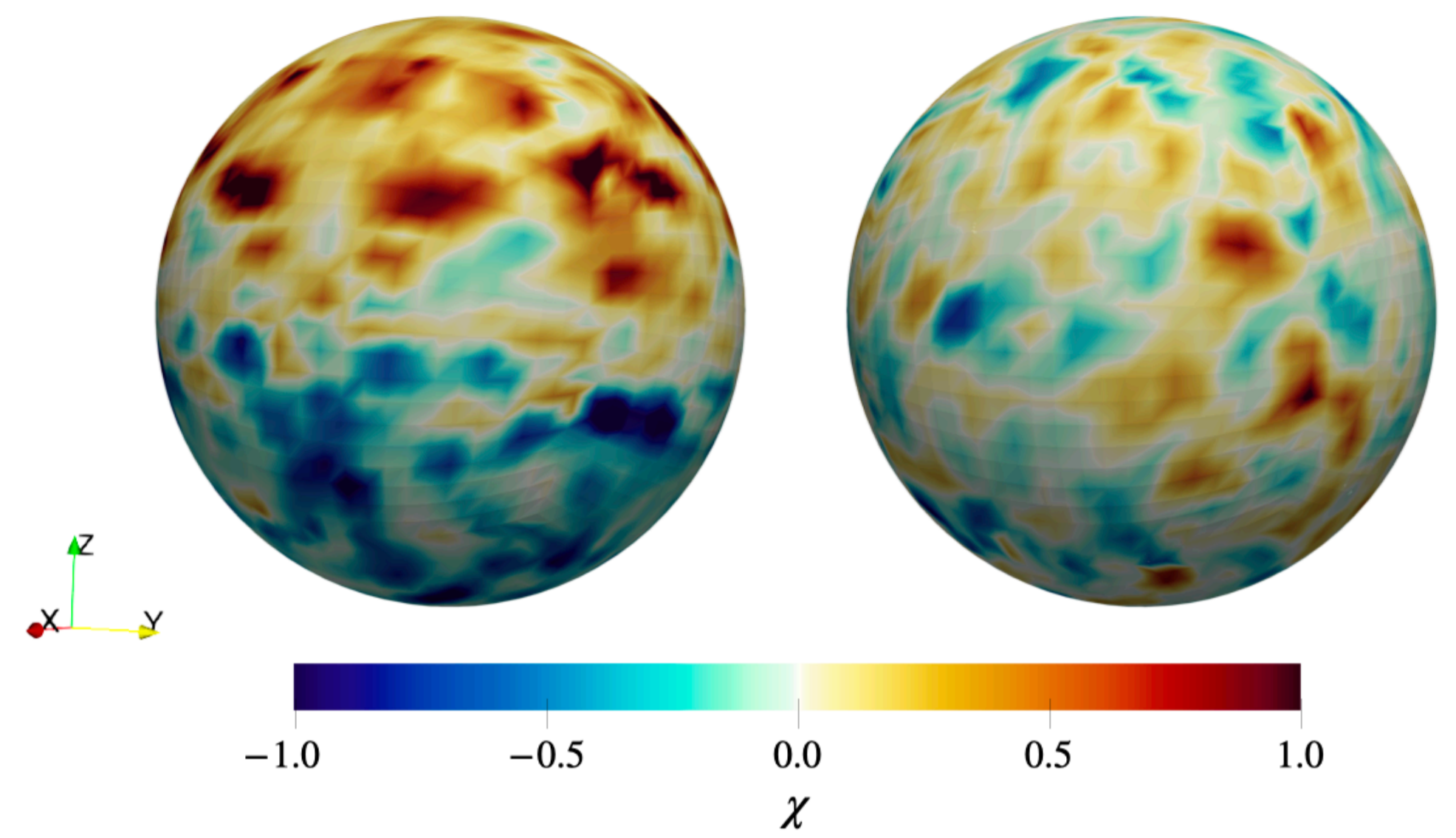
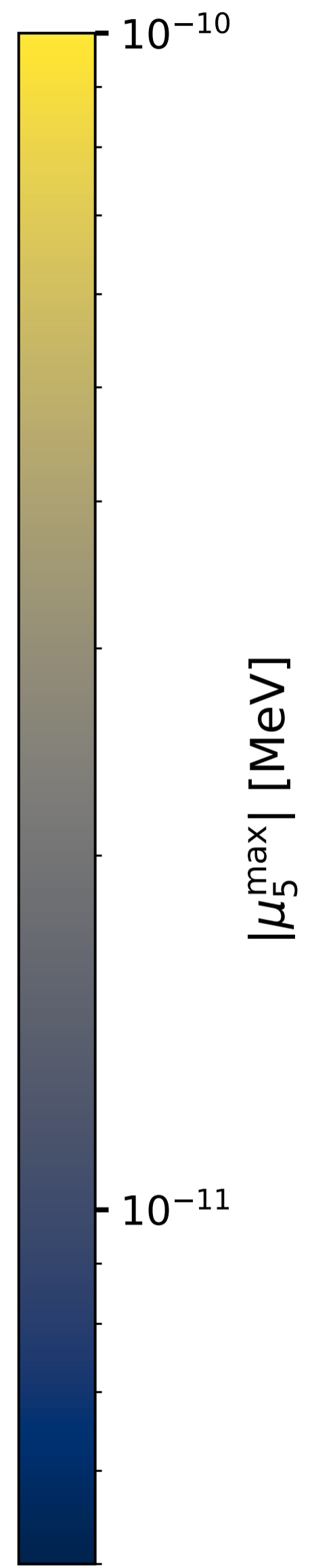
# CME simulations — vanishing helicity

Onset of CMI is governed by  $|\mu_5^{\max}|$

Magnetic energy transferred from helical modes to less helical modes



Strong helicity fluctuations drive dipolar field decay



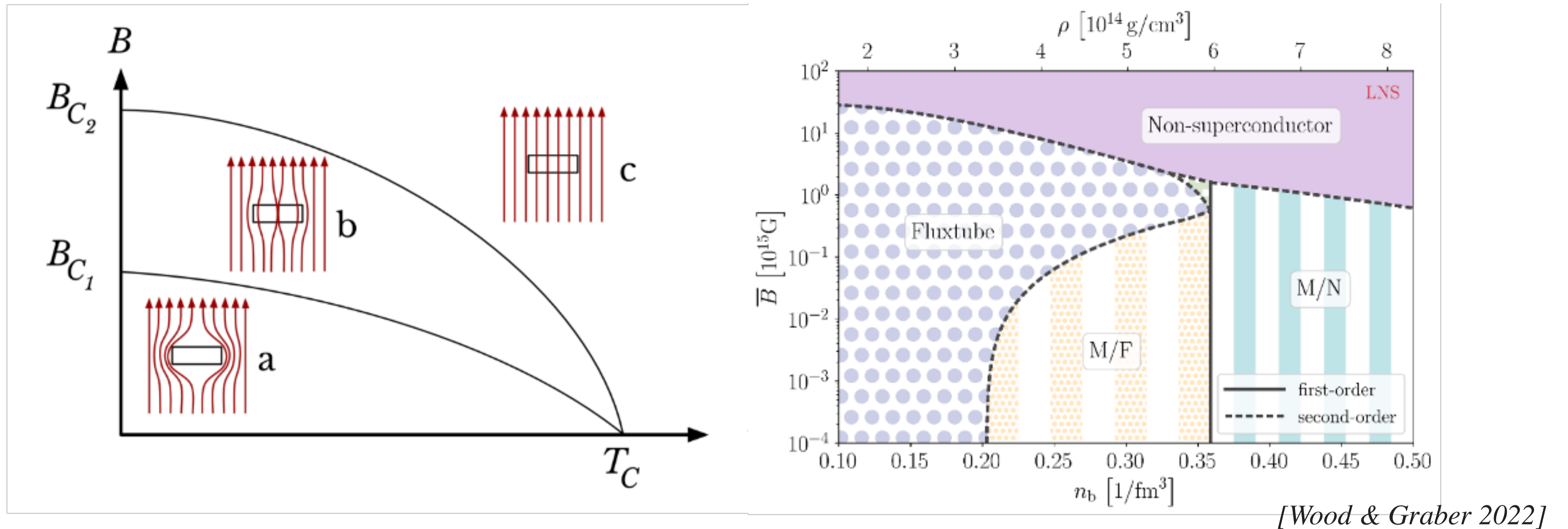
CME provides a possible explanation for magnetar formation  
 At birth: need **initial field (small scales)** + **helicity distribution**

[Dehman 2026, arXiv: 2605.08068]



# What physics is still missing?

## Magnetic field evolution in the core



In the core, physics is more complex. A mixture of neutrons, protons, electrons, muons (and others?) is expected: multi-fluid MHD  $\rightarrow$  ambipolar diffusion.

Moreover: superfluidity (neutrons) and superconductivity (protons) of type II (b), with the magnetic flux contained in tiny vortices (fluxtubes); for lower  $B$ , Meissner effect (type I, (a)).

Multi-spatial/timescale problem extremely challenging! (Gusakov et al. 2020 for a review of the current debate, and Igoshev & Hollerbach 2022 for recent results –no SC, only ambipolar diffusion–).

# How does type-II superconductivity affect field evolution in the core?

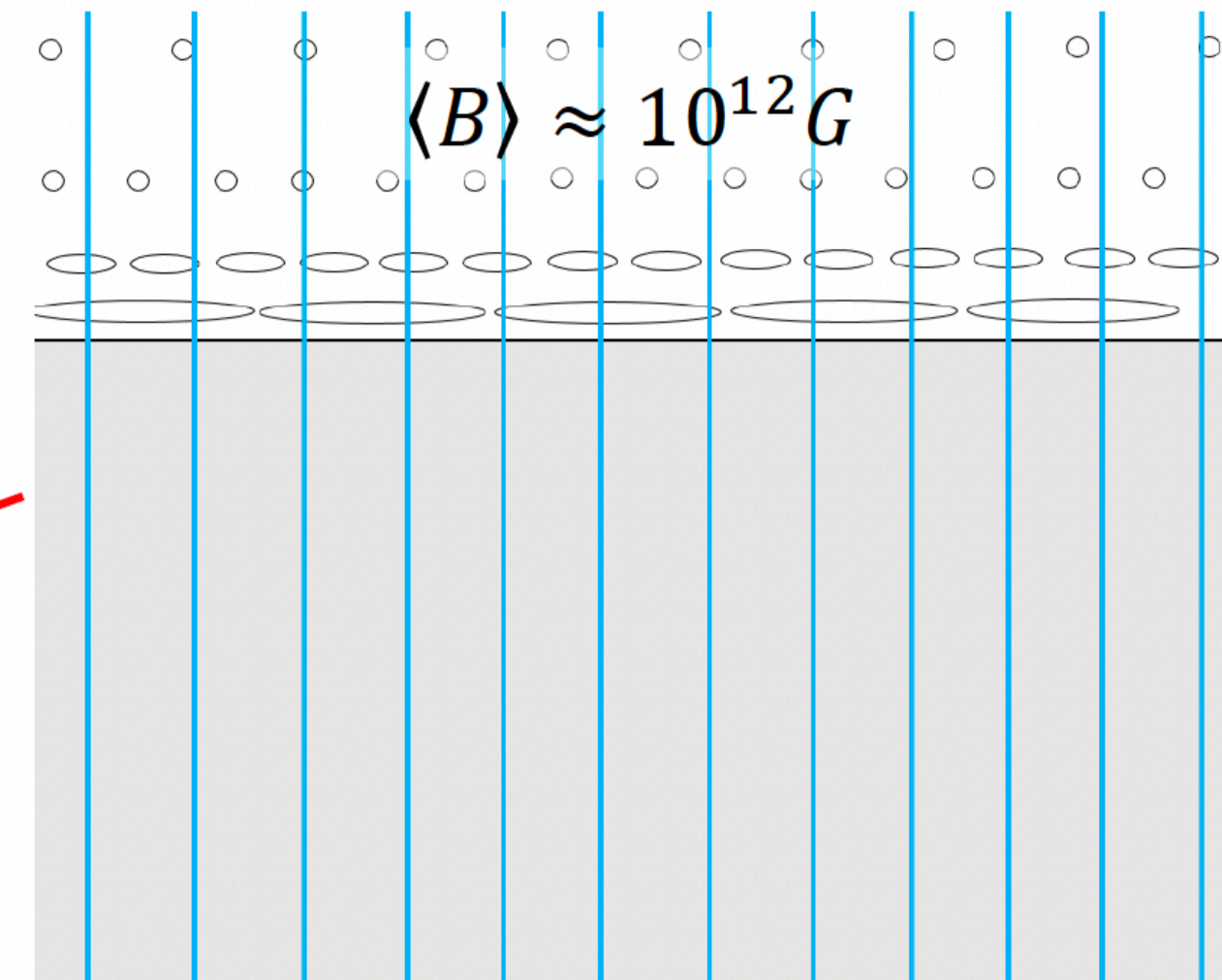
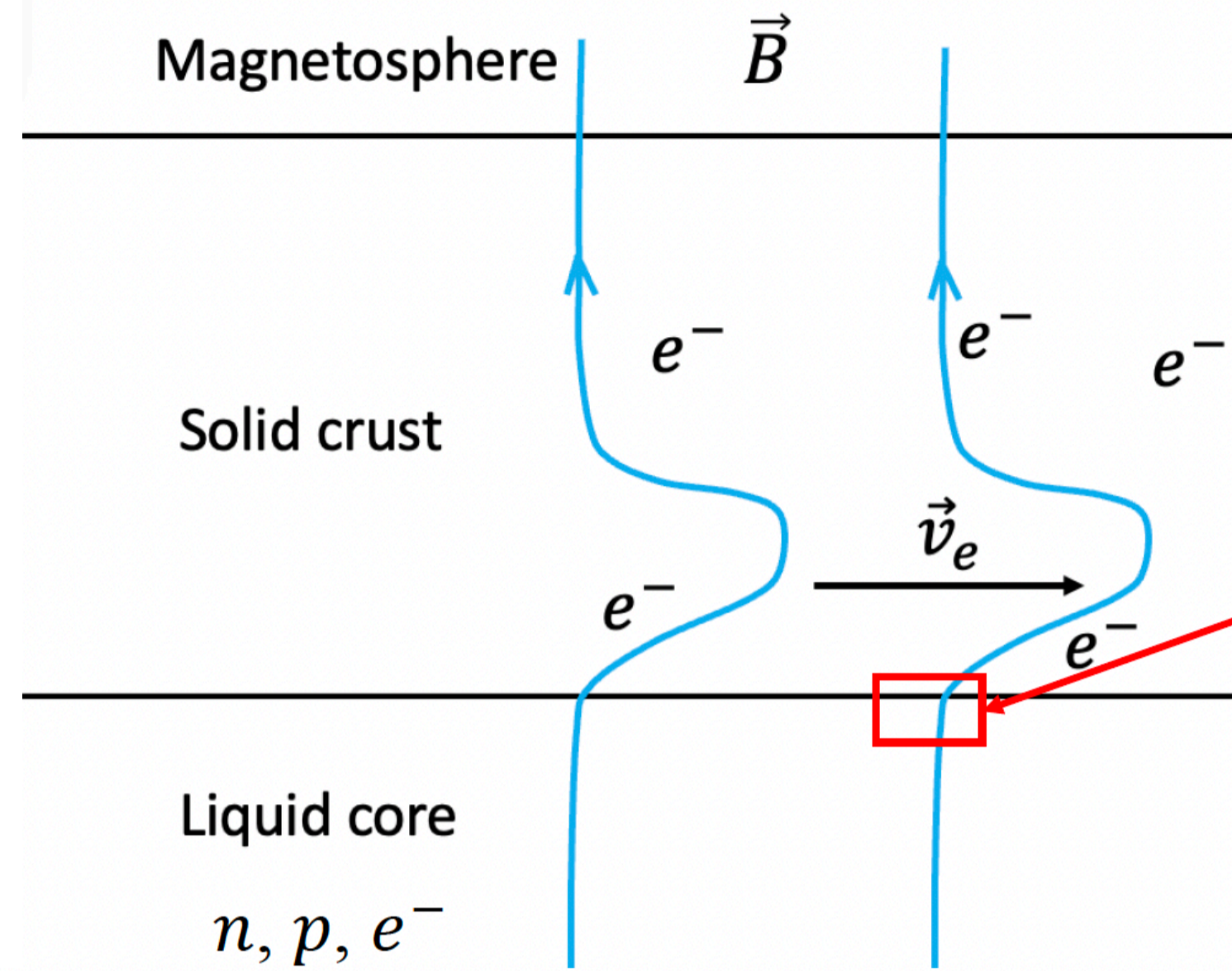
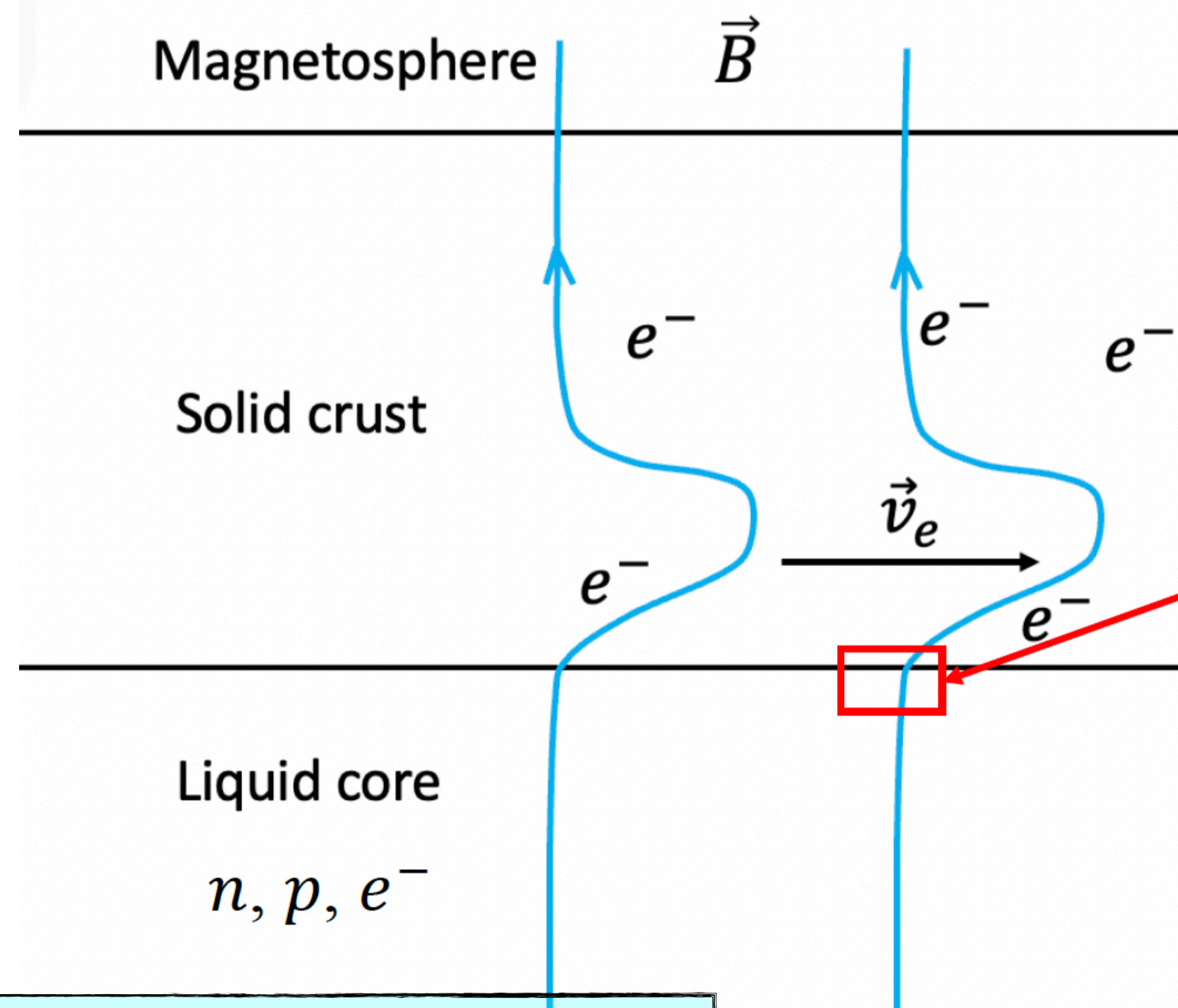
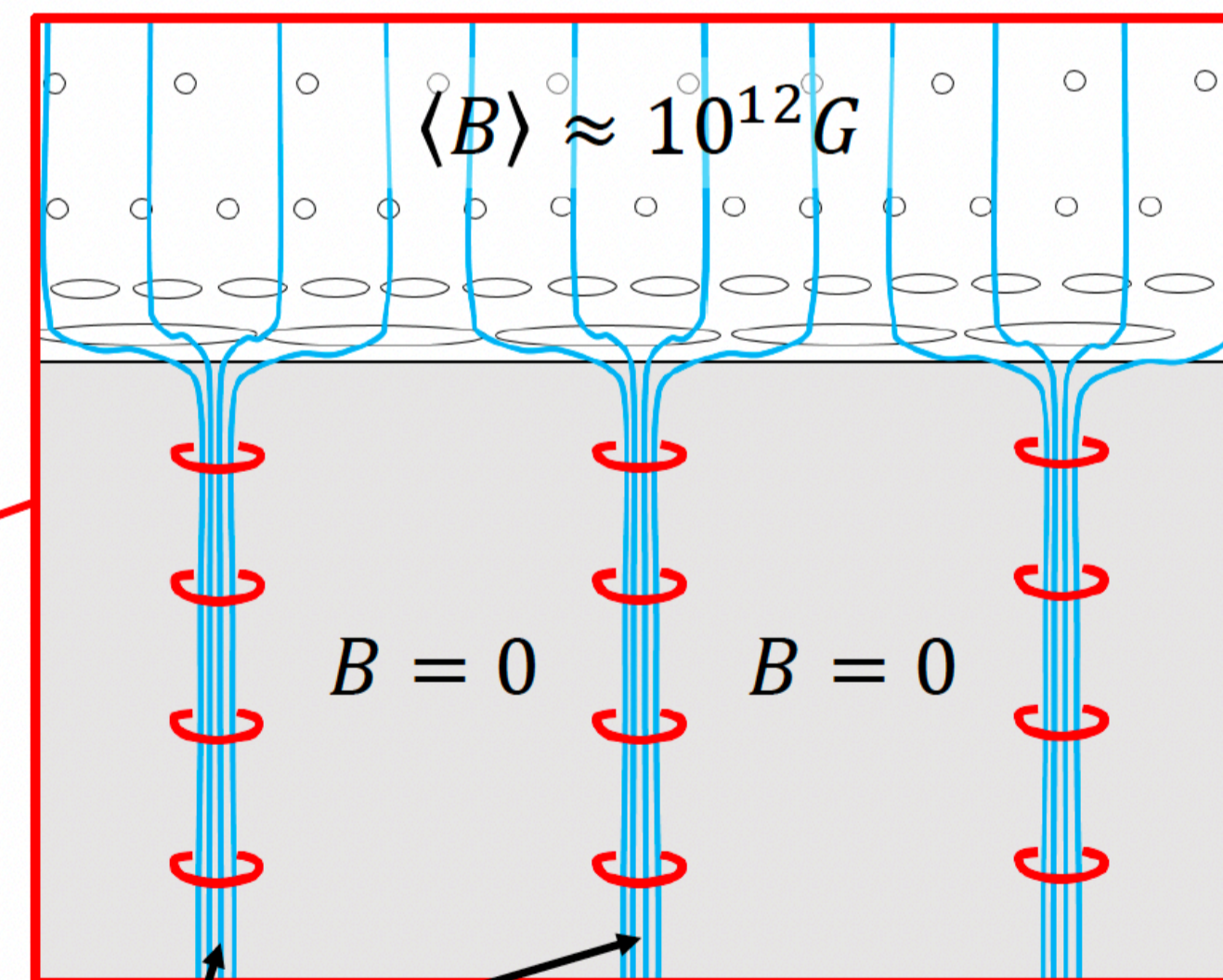


Image credit: Y. Levin



## TYPE II SUPERCONDUCTOR

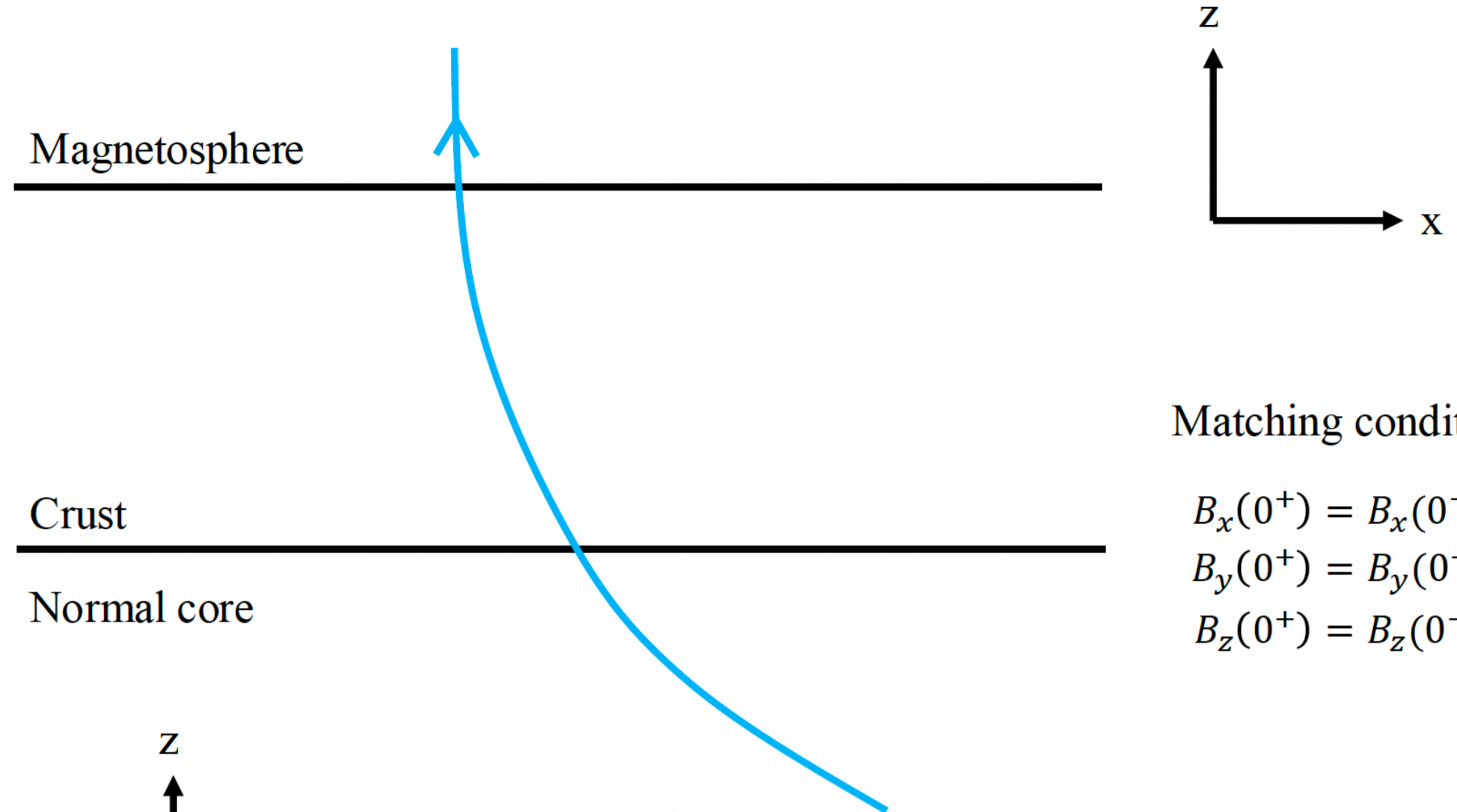


$B_{crit} \approx 10^{15} G$   $T_{crit} \approx 10^9 K$

Maxwell Stress:  $\frac{B_i B_j}{4\pi} \rightarrow \frac{B_i H_j}{4\pi}$  1000x larger

[Midgal 1959; Baym+1969; Akgun & Wasserman 2008]

# Hall-pulse launch at the crust-core interface



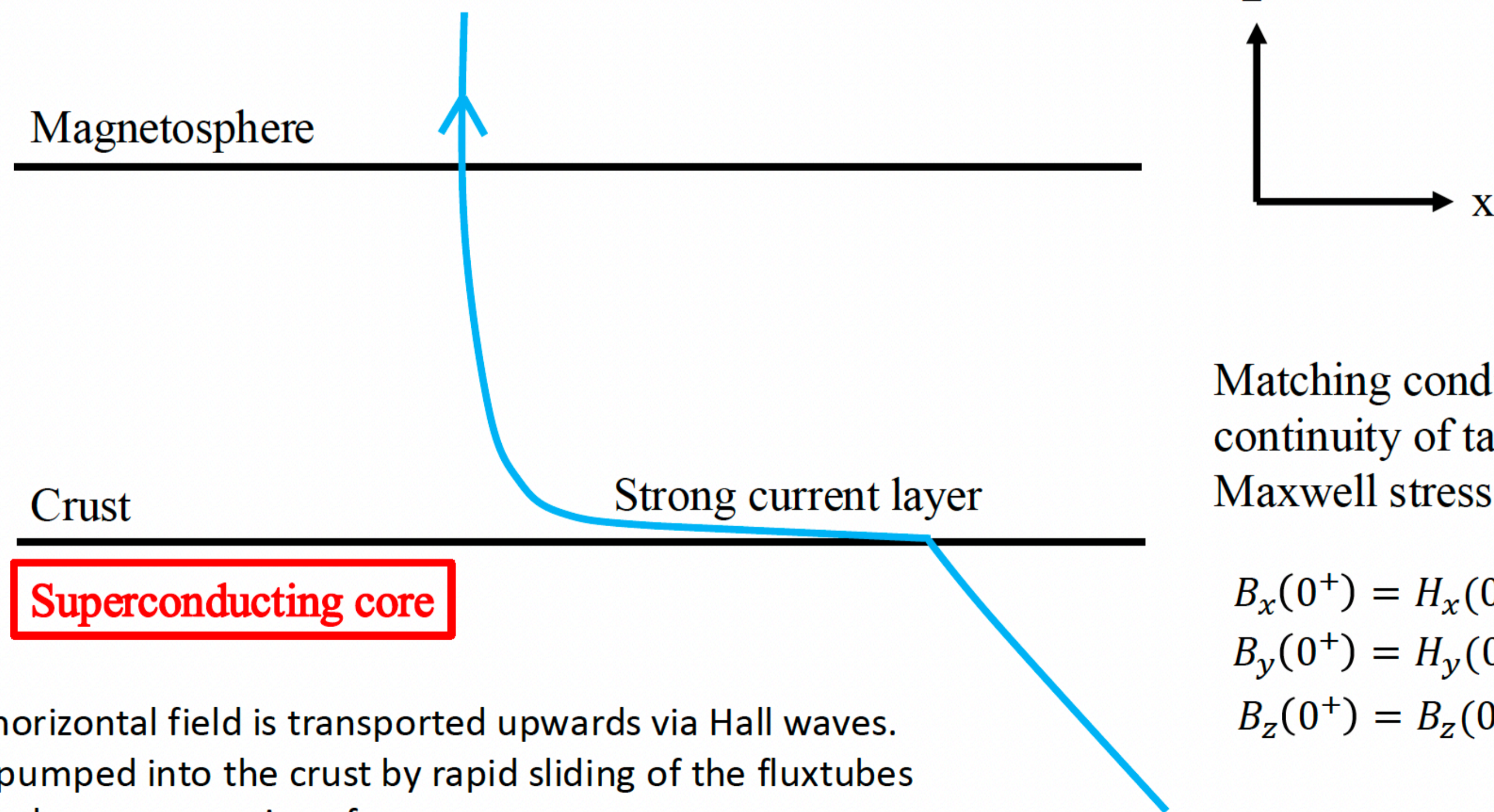
Matching conditions

$$B_x(0^+) = B_x(0^-)$$

$$B_y(0^+) = B_y(0^-)$$

$$B_z(0^+) = B_z(0^-)$$

Image credit: Y. Levin



Matching conditions:  
continuity of tangential  
Maxwell stress

$$B_x(0^+) = H_x(0^-)$$

$$B_y(0^+) = H_y(0^-)$$

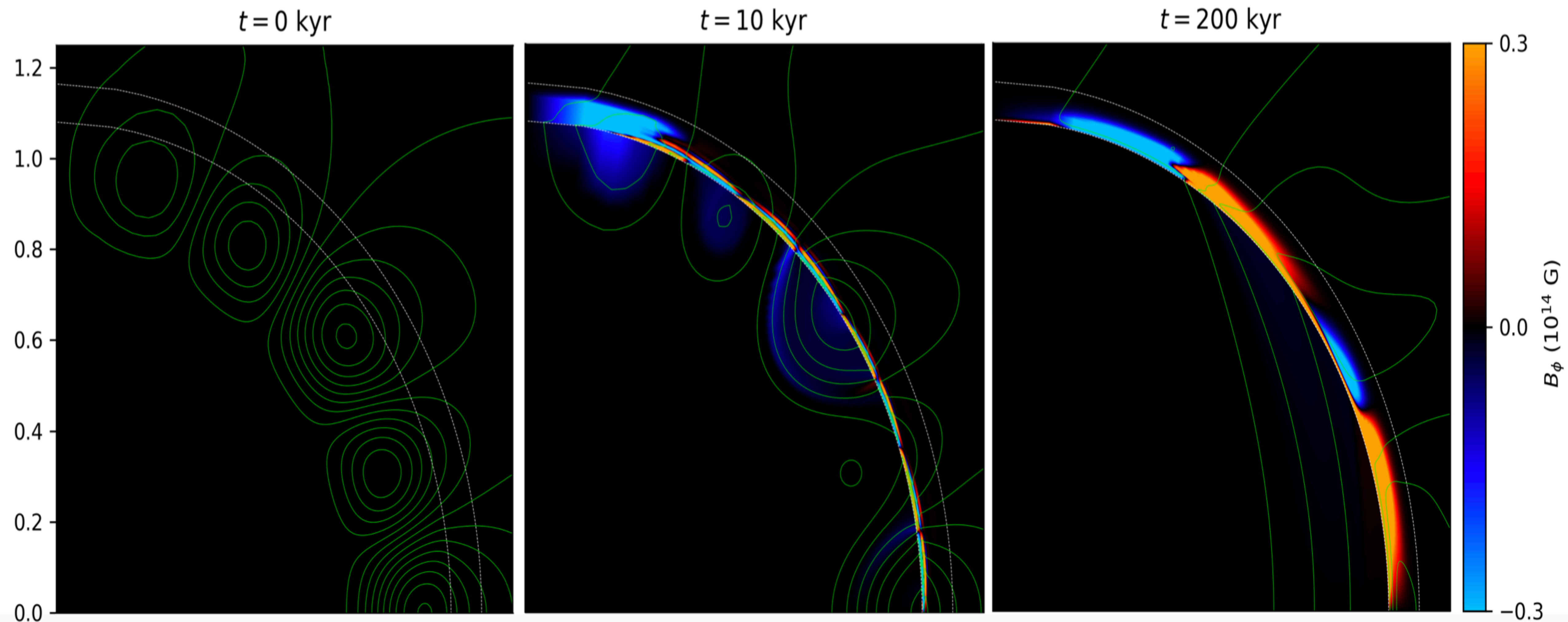
$$B_z(0^+) = B_z(0^-)$$

**Superconducting core**

The horizontal field is transported upwards via Hall waves. It is pumped into the crust by rapid sliding of the fluxtubes along the crust-core interface.

# Hall-pulse launch at the crust-core interface

— 2D simulations —



A potential candidate to explain variation in the braking index, crustal failures in the crusts of pulsars (low magnetic field with respect to magnetars).

## Summary & Conclusion:

**MATINS**: a new 3D code for magneto-thermal evolution of isolated neutron stars, enabling self-consistent Myr-scale evolution linking magnetic fields to X-ray emission, spin-down, and magnetar activity.



Long-term evolution ( $10^6$  yr) with a strong magnetic field  $\sim 10^{14} \dots 10^{15}$  G.

Proper treatments of microphysics, envelope models, axial singularity, field structure, temperature, etc.

Hall cascade, Inverse Hall cascade, outburst, etc.

### Neutron star cooling:

- Careful microphysics treatment, including superfluid and superconducting gap effects, is essential for neutron-star cooling models.
- Nuclear EOSs must activate enhanced cooling in order to explain the observations of faint yet young neutron stars.

### Magnetic field in neutron stars and magnetars:

- Dynamo simulations in core-collapse simulations and proto-neutron stars.
- Inverse cascade in neutron star
- **Chiral anomaly at the origin of magnetars large scale magnetic field.**

Including superconductivity in magnetic field evolution is essential for realistic studies.

